WIRING OF PRESYNAPTIC INHIBITORY CIRCUITRY IN THE MOUSE SPINAL CORD

A Dissertation

Presented to the Faculty of the Weill Cornell Graduate School

of Medical Sciences

in Partial Fulfillment of the Requirements for the Degree of

Doctor of Philosophy

By

Juliet Zhang

June 2016

© 2016 Juliet Zhang

WIRING OF PRESYNAPTIC INHIBITORY CIRCUITRY IN THE MOUSE SPINAL CORD

Juliet Zhang, Ph.D.

Cornell University 2016

Proper neural circuit development, organization, and function are essential to produce correctly executed behaviors. Neural circuits in the spinal cord process sensory information, and coordinate movement. One essential circuit in the spinal cord that has been well studied is the sensory-motor reflex circuit. This circuit is subject to interneuron modulation, specifically by inhibitory GABAergic interneurons, termed GABApre neurons. GABApre neurons exert presynaptic inhibition by forming synaptic boutons on sensory afferent terminals and thereby controlling sensory signaling onto motor neurons.

Previous work on GABApre neurons has identified that they express specific synaptic markers, possess stringent specificity with their sensory neuron synaptic partner, and play a role in mediating smooth movement. Deficits in presynaptic inhibition have been observed in human diseases, such as dystonia and Parkinson's disease. GABApre neurons exert presynaptic inhibition but their molecular profile and contribution to motor disease is not well known.

In this dissertation, I examine the molecular profile of GABApre neurons, and their potential link to the motor disease, dystonia. I show that the

kelch-like family member 14 (*Klhl14*) identified from a screen for genes enriched in the intermediate spinal cord, is expressed in GABApre neurons. Klhl14 directly binds the torsin family 1, member A (Tor1a) dystonia protein, which is co-expressed in GABApre neurons. Further, I show that when Tor1a is mutated in such a way that disrupts its binding with Klhl14, there is a reduction in the number of properly formed GABApre boutons, providing a link between GABApre circuitry and motor disease.

BIOGRAPHICAL SKETCH

Juliet Zhang graduated with a BA in Philosophy and minor in Natural Sciences from the University of Southern California in Los Angeles, CA in 2008. She was first exposed to an interest in neuroscience when she was a Research Assistant in the laboratory of Dr. Nathaniel Heintz at Rockefeller University in New York, NY from 2008 to 2010 before she enrolled in the Neuroscience PhD program at Weill Cornell Graduate School of Medical Sciences. Juliet was born in China, and raised in Canada before moving to the United States when she was 12.

DEDICATION

To Damion, for always being with me through the most informative years of my life. I miss you.

To Mom, for always being supportive of my dreams no matter how ambitious, and always fostering my creative and artistic side.

To Dad, for spoiling me and taking me on endless adventures.

ACKNOWLEDGEMENTS

Firstly, I would like to thank Dr. Julia A. Kaltschmidt for the being my graduate mentor and giving me the opportunity to conduct this work in her lab. Julia's guidance, attention, and compassion have been major assets towards both conducting research and writing throughout the entirety of my PhD. She has always impressed upon me her dedication and hard work. I would also like to thank past and present members of the lab- Jarret Weinrich for the screen for intermediate enriched genes, contributions to synaptic analyses, discussion on dystonia and helpful advice, Josephine Belluardo for technical assistance, helpful discussion and encouragement, Richard DiCasoli for technical assistance and always being willing to help, Danny Comer for data analysis, discussion on developmental timing and sharing wisdom, Praveen Bommareddy for technical assistance and being supportive, Aanchal Tyagi for technical assistance, and Jeff Russ for preliminary timing data. I would like to thank the Bioinformatics core at MSKCC for data analysis. I am very grateful to my thesis committee- Dr. M. Elizabeth Ross, Dr. Tao Sun, and Dr. Leslie B. Vosshall- for their guidance and encouragement throughout my graduate training.

Finally, I want to thank my parents and family for all the love and support, and always believing in my success. I want to thank Brian Haley for being an amazing partner in every which way imaginable. I also want to thank all my friends- both human and cat friends alike- having such a close community has always been invaluable.

TABLE OF CONTENTS

LIST OF FIGURES

LIST OF ABBREVIATIONS

ATP ..... adenosine triphosphate
BMP ..... bone morphogenetic protein
BrdU ..... bromodeoxyuridine
Caspr4 ..... contactin associated protein-like 4
Chl1 ..... contactin adhesion molecule L1-like
Cm ..... cutaneous maximus
CNS ..... central nervous system
Cre ..... cre recombinase
Cre^{ER} ..... cre recombinase fused to estrogen receptor
Crym ..... crystallin, mu
CST ..... corticospinal tract
Dyt1ΔE ..... Tor1a with a single glutamic acid deletion
DRG ..... dorsal root ganglia
DT .....diphtheria Toxin A
Dyt1 ..... torsin family 1, member A / dystonia 1 protein
e ..... embryonic day
EM ..... electron microscopy
EPSP ..... excitatory post-synaptic potential
ER ..... endoplasmic reticulum
Er81 ..... ets variant 1
FACS ..... fluorescence-activated cell sorting
FoxP1 ..... forkhead homeobox P1
GABA ..... γ-aminobutyric acid
GAD ..... glutamic acid decarboxylase
GDNF ..... glial cell line-derived neurotrophic factor
GFP ..... green fluorescent protein
HRP ..... horse radish peroxidase
IaIN ..... Ia inhibitory interneuron
Klhl14 ..... kelch-like family member 14
KO ..... knockout
Lbx1 ..... ladybird homeobox 1
LMC ..... lateral motor column
MN ..... motor neuron
NB2 ..... contactin 5

NE ..... nuclear envelope
NMJ ..... neuromuscular junction
NPY ..... neuropeptide Y
NrCAM ..... neuronal cell adhesion molecule
p ..... postnatal day
PAD ..... primary afferent depolarization
Pea3 ..... ets variant 4
pENK ..... enkephalin
PFA ..... paraformaldehyde
Plxnd1 ..... plexin D1
pMN ..... motor neuron progenitors
Ptf1a ..... pancreas transcription factor 1a
Pv ..... parvalbumin
RC..... Renshaw cell
RFP.....red fluorescent protein
RT-PCR ..... reverse transcription Polymerase Chain Reaction
SD ..... standard deviation
SEM ..... standard error of the mean
Sema3e ..... semaphorin 3e
Shh ..... sonic hedgehog
Syt1 ..... synaptotagmin-1
Tfap2β..... transcription factor AP-2 beta
Tlx ..... T-cell leukemia homeobox
TM ..... tamoxifen
Tor1a ..... torsin family 1, member A / dystonia 1 protein
Tri ..... triceps
vGluT1 ..... vesicular glutamate transporter-1
wt ..... wild-type
YFP ..... yellow fluorescent protein

LIST OF SYMBOLS

β ..... beta
Δ ..... delta
γ ..... gamma
μ ..... micro
V ..... volume

Chapter 1

Spinal motor circuit assembly and potential role in motor disease

1.1 Introduction

The ability of an organism to acquire information, process it, and interact successfully with its environment is dependent on the proper functioning of its central nervous system (CNS). The CNS consists of the brain and spinal cord, which relay information through neural circuits and synapses. In order for neural circuitry to wire correctly, an extremely high level of organization and precision is required. Even the slightest perturbation to this system can lead to neurological deficits and disease, such as schizophrenia and multiple sclerosis.

In order to understand neurological diseases and determine how to ameliorate and cure them, it is essential to first understand how the nervous system functions. Understanding neural circuitry formation and how its component neurons form synaptic contacts and maintain them is a complex, multi-faceted question in neuroscience. Historically, circuits in the spinal cord that control motor behavior have served as an excellent system to probe this question.

1.2 Motor neuron organization

In the spinal cord, three fundamental neuronal classes are essential for controlling motor behavior. Motor neurons, sensory neurons and interneurons

play unique roles in facilitating movement. Motor neurons form specialized synapses called neuromuscular junctions (NMJ) onto muscles. Upon neurotransmitter release from the NMJ, the muscle is triggered and movement results (Amin et al., 2015).

Motor neuron cell bodies reside within the ventral spinal cord (ventral horn), and their projections extend great distances throughout the organism to contact discrete muscles. The positioning and connectivity of motor neurons is highly orchestrated and precise. Motor neurons target muscles with distinct functions, such as flexors or extensors. Flexor muscles contract and decrease the angle of a joint, such as the biceps bending the elbow joint. Extensors contract and extend, which increases the angle on a joint, such as the triceps straightening the elbow joint. How motor neurons are organized, develop, and target distinct muscle groups have been heavily studied topics in neuroscience.

Some of the first work that began to elucidate motor neuron organization was performed by George Romanes in 1951 (Romanes, 1951). He combined histological visualization and selective muscle denervation to explore motor neuron organization and innervation of specific muscles in the mammalian hindlimb. By crushing specific nerves in the hindlimb of the cat, he was able to trace the nerves back to chromatolytic, or injured, neurons in the spinal cord, thereby identifying the position of motor neurons in relation to specific muscle innervation (Romanes, 1951). Romanes found that motor neurons cluster into functionally related groups, which he named “motor pools” (Fig. 1.1A). Motor neurons within a motor pool innervate a single muscle. Motor pools are positioned along a finite rostrocaudal extent of the spinal cord,

which are called motor columns (Romanes, 1951). The precise positioning of these columns within the dorsoventral, mediolateral and rostrocaudal axes of the spinal cord topographically corresponds to the location of their targets in the periphery (Sürmeli et al., 2011). For example, in the lateral motor column (LMC) whose motor neurons innervates limbs, the medial LMC motor neurons target the ventral part of a limb and the lateral LMC motor neurons target the dorsal part of the limb (Fig. 1.1B, Stifani, 2014).

More recently, dyes have been used as tracers to backfill motor neuron cell bodies from limb muscles. The injection of horseradish peroxidase (HRP) into limb muscles retrogradely labels motor neurons, and allows for a clear visualization of their cell bodies in the spinal cord. In addition, fluorescent signal amplification of such tracers used to backfill motor neurons along with immunohistochemistry methods has allowed for a near complete assessment of motor pool organization (McHanwell and Biscoe, 1981; Lin et al., 1998; Sürmeli et al., 2011).

1.2.1 Motor neuron development

Neuronal positioning and differentiation in the developing spinal cord is directed by two secreted signaling sources, sonic hedgehog (Shh) and bone morphogenetic protein (BMP), that form gradients along the dorsoventral axis. Shh is expressed ventral-high and dorsal-low, while BMP is expressed oppositely, dorsal-high and ventral-low (Jessell, 2000; Liem et al., 2000).

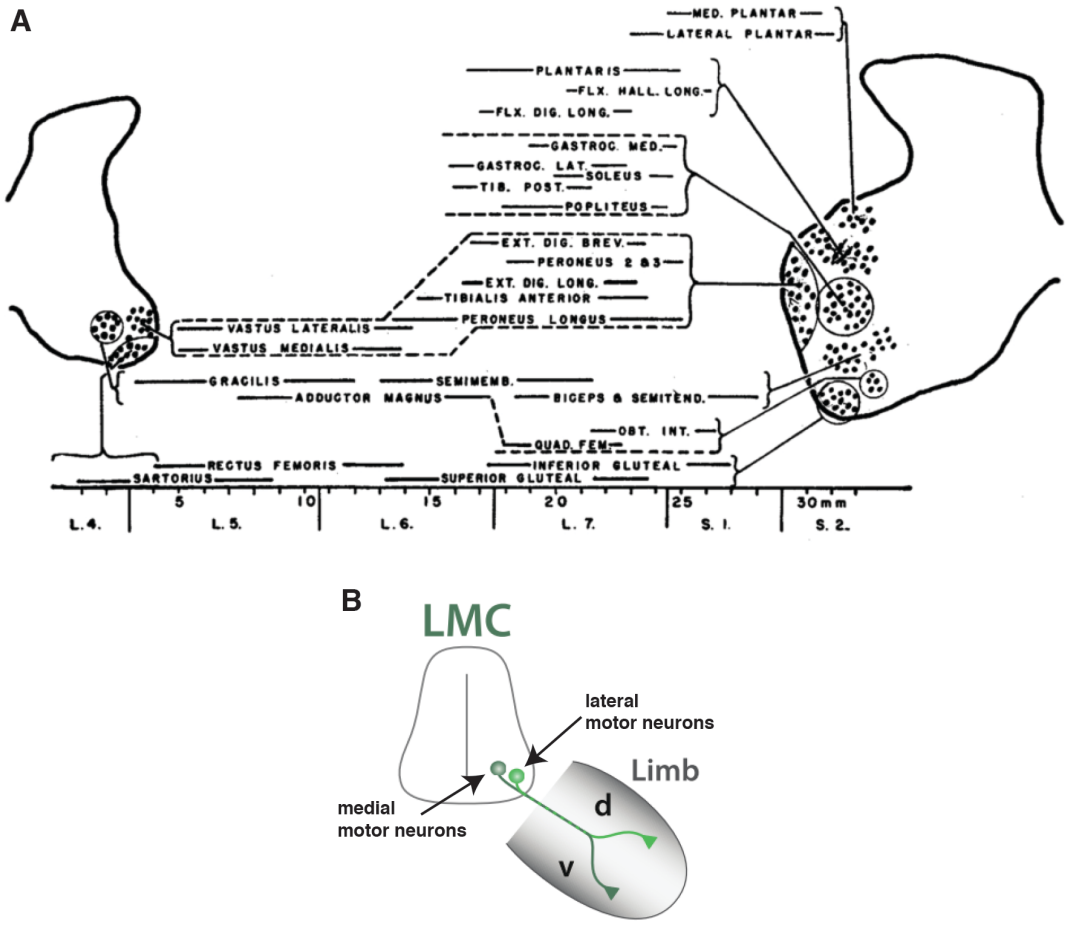

Figure 1.1: Motor neuron organization

(A) Drawing from George Romanes showing motor neurons organized by pool, and extending into columns along the rostrocaudal axis. Functionally related motor neurons that innervate the same muscle are clustered together in distinct motor pools. From Romanes, 1951.

(B) Motor neuron positioning in the spinal cord corresponds to motor neuron projections in the periphery. In the LMC, lateral motor neurons innervate the dorsal part of the limb, whereas the medial motor neurons innervate the ventral part of the limb. Adapted from Stifani et al., 2014.

These inductive signals, followed by the expression of specific homeodomain proteins, determine 11 specific progenitor domains that occupy discrete dorsoventral positions (Briscoe et al., 2000; Gross et al., 2002; Müller et al., 2002). Six of these domains are dorsal, and five are ventral (Fig. 1.2, Jessell, 2000; Alaynick et al., 2011; Zeilhofer et al., 2012). The progenitor domains extend throughout the rostrocaudal extent of the organism, and precursors within the domains give rise to postmitotic neurons during development. Motor neurons require a high concentration of Shh protein to be induced (Roelink et al., 1995; Ericson et al., 1996; Liem et al., 2000). The ventral pre-motor neuron (pMN) domain gives rise exclusively to motor neuron precursors beginning on embryonic (e) day e9.5 (Hollyday and Hamburger, 1977; Nornes and Carry, 1978).

Motor neurons begin innervating their muscle targets at e11.5, while their cell bodies are grouped in pools and coupled electrically by gap junctions, which are intercellular connections that enable cells to share electrical impulses and eventually fire together (Chang et al., 1999; Hanson and Landmesser, 2003). The timing of motor neurons sending out projections to the periphery correlates with the initial expression of the Ets family transcription factors in motor neurons. Ets variant 4 (*Pea3*) is one of these factors and is expressed in subsets of motor neurons within the LMC during early development (Livet et al., 2002). *Pea3* expression is induced by glial cell line-derived neurotrophic factor (GDNF) expression in the developing forelimb and trunk (Haase et al., 2002). The expression of *Pea3* in motor neurons is necessary for their proper cell body positioning, and axon targeting and branching. In a *Pea3* mutant mouse, early neuronal identity is maintained, but

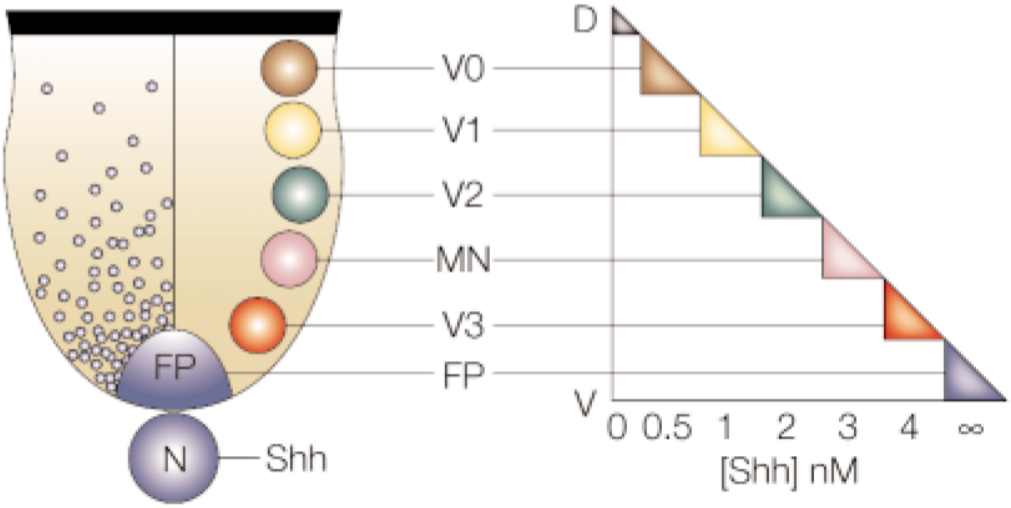

Figure 1.2: Ventral progenitor domains

Shh protein concentration is graded from the floor plate (FP) and is followed by the expression of homeodomain proteins resulting in five progenitor domains. V0-V3 domains gives rise to heterogeneous populations of ventral interneurons, and the pMN (MN) domain gives rise exclusively to motor neurons. From Jessell, 2000.

the later steps of motor pool identity are affected. In *Pea3* mutant mice, motor neurons that usually express Pea3 in the lateral motor column (LMC) shift from a ventral position to an abnormal dorsal position. Although axonal projections of these mispositioned motor neurons invade the limbs, they fail to invade into their muscle target areas and to branch (Livet et al., 2002; Vrieseling and Arber, 2006).

1.3 Sensory neuron development

While motor neurons activate muscles to induce movement, they also require proper sensory feedback, which is provided by sensory neurons. Sensory neurons are neural crest derived, and their cell bodies reside in the dorsal root ganglion (DRG), adjacent to the spinal cord. Sensory neuron projections extend into the spinal cord, and to the periphery (Brown, 1981). Sensory neurons are born at e10.5 and begin targeting muscles around e12.5, following motor neuron generation and targeting (Ozaki and Snider, 1997). After targeting the periphery, sensory neurons begin their ingrowth into the spinal cord at around e14 (Ladle et al., 2007).

There are three major classes of sensory neurons: mechanoreceptors, nociceptors, and proprioceptors. The different classes of sensory neurons communicate different sensory modalities, and participate in distinct neural circuits within the spinal cord. Mechanoreceptors sense touch and innervate the skin in the periphery, wrapping around hair follicles (Abraira and Ginty, 2013). They project into the dorsal horn of the spinal cord terminating in the deeper laminar layers including layer III, IV, and V. Nociceptors sense temperature and pain in the periphery, and project into the dorsal horn where

they terminate in superficial laminar layers I and II (Todd, 2010). The third class of sensory neurons, proprioceptors, sense the placement of limbs in space (Fig. 1.3, Caspary and Anderson, 2003). Two main classes of proprioceptors are Ia afferents and Golgi tendon organs (Ib afferents). Ia afferents extend projections into the periphery innervating muscle spindles, which sense the stretch of the muscle (Brown and Fyffe, 1981), while Ib afferents terminate at tendons where they sense muscle tension. The central projections of proprioceptors relay information into the spinal cord at two termination zones: dorsal projections into lamina V form contacts onto interneurons, and ventral projections form contacts onto motor neurons (Eccles et al., 1957; Burke and Nelson, 1966; Brown and Fyffe, 1981).

The developmental timing of when proprioceptive neurons project into the spinal cord involves molecular cues from the periphery. By removing the hindlimb and therefore neurotrophic factors in the periphery, Ets variant 1 (*Er81*), a member of the Ets transcription family is no longer expressed in sensory neurons (Lin et al., 1998). This loss of *Er81* in proprioceptors leaves their dorsal spinal projections intact, but results in the failure of proprioceptors to extend ventrally into the spinal cord (Arber et al., 2000). This sensory projection phenotype is also recapitulated in *Er81* mutant mice, which exhibit a severe motor phenotype such as loss of limb control and motor coordination. (Arber et al., 2000).

1.4 Sensory-motor reflex circuit

Proprioceptors and motor neurons together participate in the monosynaptic reflex circuit, which contracts a muscle in response to muscle

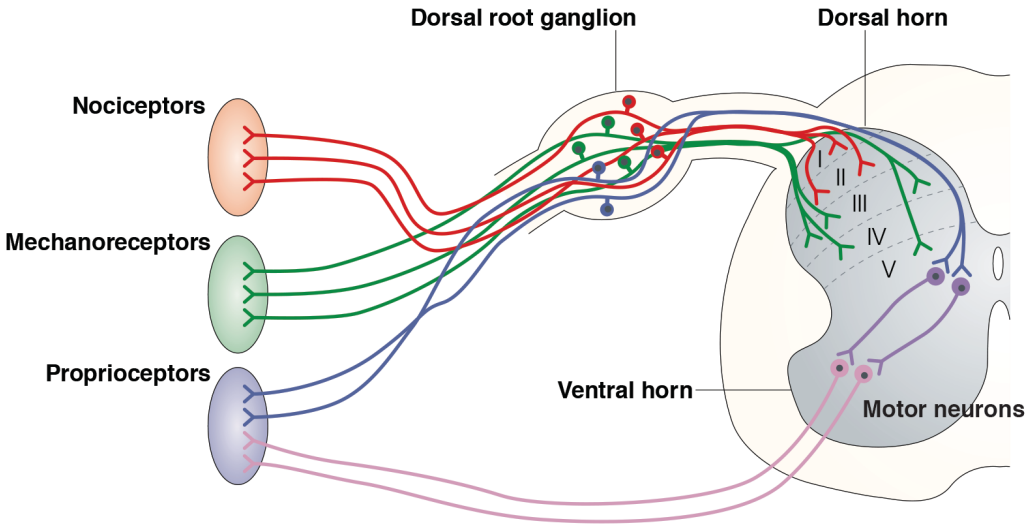

Figure 1.3: Major classes of sensory neurons

There are three major classes of sensory neurons: nociceptors, mechanoreceptors, and proprioceptors. Sensory neuron cell bodies are located in the dorsal root ganglion (DRG), and different classes of neurons project into different lamina of the spinal cord. Proprioceptors project into two regions of the spinal cord: dorsally in lamina V, and ventrally where proprioceptive afferents form contacts onto motor neurons. Adapted from Caspary and Anderson, 2003.

stretch (Fig. 1.4). This simple two-neuron circuit has served as an excellent model to understand synaptic specificity. Proprioceptive sensory neurons almost exclusively contact motor neurons that project to the same muscle in the periphery. This sensory-motor pairing happens less in muscles that have the same function (heteronymous muscles), and is almost negligible in muscles that have different functions (antagonistic muscles) (Eccles et al., 1957; Mears and Frank, 1997).

Different mechanisms have been described to ensure that sensory neurons form synapses onto the correct motor neuron partner, and avoid the incorrect ones. One way that sensory neurons avoid incorrect motor neuron partners is to respond to repellent cues. The motor neurons of the cutaneous maximus (Cm) do not receive any direct proprioceptive contacts, and they achieve this by expressing a class 3 semaphorin (Sema3e). Sensory neurons that express the high-affinity receptor of Sema3e, Plexin D1 (Plxnd1), recognize this cue and avoid contacting Cm motor neurons. In *Sema3e* mutant mice, Cm motor neurons do receive proprioceptive input from Ia afferents. Furthermore, ectopic expression of Sema3e in the motor neurons of the triceps (Tri) that usually receive proprioceptive input greatly reduces the number of proprioceptive contacts on them (Pecho-Vrieseling et al., 2009; Fukuhara et al., 2013). The proper expression of Sema3e in distinct subsets of motor neurons and expression of Plxnd1 in a subset of sensory neurons reveals that repulsive molecular cues are essential for proper sensory-motor connectivity.

Besides molecular mechanisms, proper sensory-motor connectivity also requires proper cell body positioning of motor neurons in the spinal cord. In

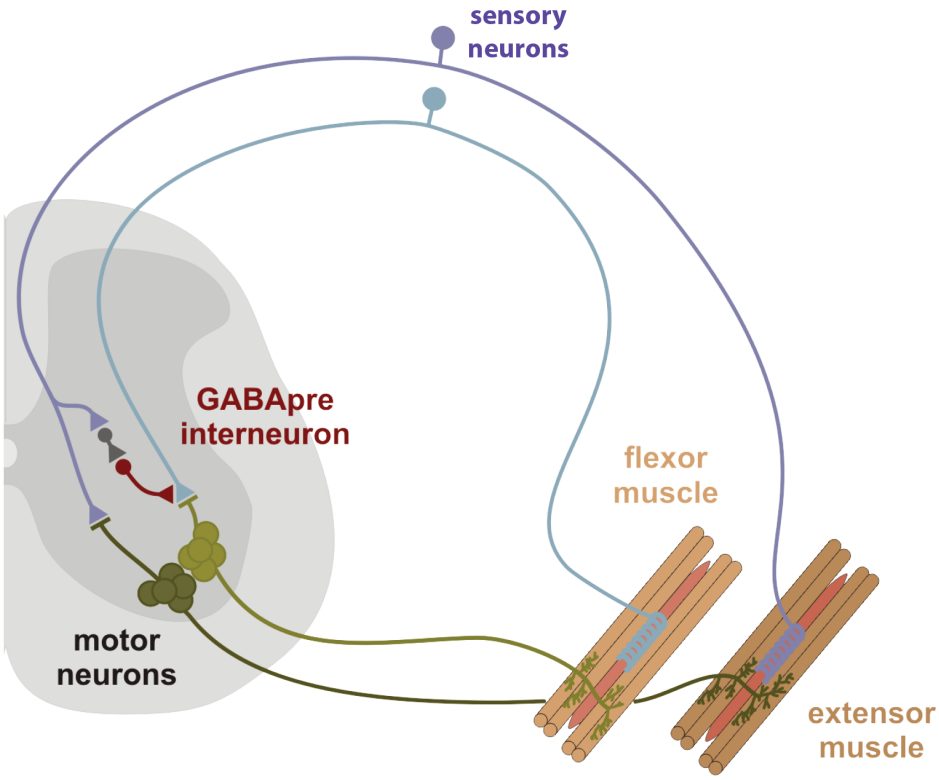

Figure 1.4: The monosynaptic reflex circuit

The monosynaptic reflex circuit consists of a sensory afferent that forms a spindle on a muscle and senses stretch in that muscle, and projects into the spinal cord where it forms a terminal on a motor neuron. The motor neuron projects back into the same muscle as the sensory neuron. GABApre neurons mediate presynaptic inhibition by forming an axo-axonic contact on the sensory terminal. Adapted from Betley et al., 2009.

mutant mice in which motor pool specification is lost due to loss of forkhead box P1 (*FoxP1*), motor neurons have a scrambled cell body positioning. Interestingly, the sensory neurons in *FoxP1* mutant mice still project to the physical location of where specific motor pools should have been and form aberrant contacts onto the scrambled motor neurons residing there (Sürmeli et al., 2011). Together, these studies suggest that sensory neurons rely on both molecular cues as well as motor neuron positioning to find their proper synaptic partners.

1.5 Interneuronal diversity and development

In the spinal cord, interneuron populations span the entire length of the spinal cord, and reside in both the dorsal horn as well as the ventral horn. Interneurons are extremely heterogeneous and their diversification is reflective of the complexity necessary for neural circuits to produce behavior. A major goal in neuroscience has been to identify and specifically study subpopulations of interneurons throughout the CNS (Jankowska, 2001; Zeilhofer et al., 2012; Kepecs and Fishell, 2014).

How does interneuron diversity arise in the spinal cord? Interneuron diversity begins embryonically with three ventral progenitor domains that give rise to different classes of ventral interneurons, V0-V3, and six dorsal progenitor domains that give rise to different classes of dorsal interneurons, dI1-6 (Jessell, 2000; Helms et al., 2005). Each domain gives rise to several different neuronal subtypes that express unique sets of transcription factors to determine their unique identity (Arber, 2012). For example, the dI4 domain expresses pancreas specific transcription factor 1a (*Ptf1a*) and gives rise to

dorsal inhibitory interneurons, whereas the dI5 domain expresses transcription factors T-cell leukemia homeobox 1 (*Tlx1*) and *Tlx3* and gives rise to dorsal excitatory interneurons (Helms and Johnson, 2003).

Subpopulations of spinal interneurons can be excitatory or inhibitory, primarily using glutamate if excitatory, and γ-aminobutyric acid (GABA) or glycine if inhibitory. The acquisition of inhibitory interneuron fate in the dorsal spinal cord is necessary and dependent on *Ptf1a*. Without the expression of *Ptf1a*, interneurons that should have assumed an inhibitory fate, switch to an excitatory fate (Glasgow et al., 2005). Excitatory interneuron fate in the dorsal spinal cord is dependent on *Tlx1* and *Tlx3*, which suppress GABAergic differentiation (Cheng et al., 2004). These opposing transcriptional networks suggest that there is a balance between factors that confer inhibitory fates and excitatory fates in the spinal cord.

1.6 Temporal regulation contributes to interneuron identity

Interneurons in the spinal cord are born between e9 to e14.5 (Matise and Joyner, 1997; Gross et al., 2002; Müller et al., 2002). The timing of birth of interneurons has been used to analyze and differentiate between the eventual identities of certain interneuronal subpopulations (Tripodi et al., 2011; Benito-Gonzalez and Alvarez, 2012).

In the dorsal spinal cord, ladybird homeobox 1 (*Lbx1*) is a transcription factor expressed in domains dI4-dI6. dI4 and dI5 cells separate into two waves of early and late-born interneurons. In early neurogenesis, the dI4 and dI5 domains are discretely positioned neighboring stripes giving rise exclusively to

inhibitory and excitatory neurons respectively. In late neurogenesis dI4 becomes the new domain dILA, and dI5 becomes the new domain dILB, with progenitors occupying the new domains in a salt and pepper fashion. Although both early and late cells express the same factor *Lbx1*, they additionally express different transcription factors and have different cell fates (Gross et al., 2002; Müller et al., 2002). Timing of birth also contributes to interneuron cell fate in the ventral spinal cord. Two types of ventral premotor interneurons are Renshaw cells (RC) that mediate recurrent inhibition on motor neurons and Ia inhibitory interneurons (IaIN) that mediate reciprocal inhibition on motor neurons. While both RCs and IaINs are born from progenitors in the V1 domain, RCs are born early (e9.5-e10.5) and IaINs are born later (e11.5-e12.5) (Benito-Gonzalez and Alvarez, 2012; Stam et al., 2012).

Identifying interneuronal subpopulations by timing of birth has enabled analysis of their neuronal circuitry and function. Tripodi et al. (2011) used labeling neurons based on timing of neurogenesis to distinguish between subpopulations of premotor interneurons. They showed that interneurons that form direct contacts with flexor motor neurons have lateral cell body positioning in the spinal cord and are born early, at e10.5. Those that contact extensor motor neurons have a medial cell body positioning and are born later, at e12.5. Tripodi et al. (2011) used a mutant animal in which proprioceptors are killed (Pv^{DTA}) and both dorsal and ventral termination zones of proprioceptors are absent, and found that cell body positioning and connectivity of the later born extensor premotor neurons was perturbed, and resembled those of the flexor premotor population. In *Er81* mutant mice in which proprioceptive connectivity is perturbed only in the ventral horn, but not

in the dorsal spinal cord, both flexor and extensor premotor interneuron distributions remained the same. Taken together, these data show that the spatial segregation and projection pattern of a subset of premotor interneurons depends on sensory input (Tripodi et al., 2011).

1.7 Premotor interneuron circuitry

The molecular identity of a specific interneuron is an important factor determining which neural circuits the neuron ultimately participates in. Two types of premotor neurons that have provided insight into interneuronal circuitry are RCs and IaINs. Both cell types are developmentally derived from the same lineage in the ventral progenitor domain V1 (Alvarez et al., 2005) and form contacts onto motor neurons, however, they participate in different neuronal circuits. IaINs form contacts onto antagonistic motor pools, providing reciprocal inhibition (Jankowska, 1992), whereas RCs contact synergistic motor neurons, providing recurrent inhibition. During development, both RCs and IaINs receive direct contacts from group Ia proprioceptive afferents. However the direct sensory contacts on RCs are transient, weakening after p15; while, those on IaINs strengthen to adulthood (Mentis et al., 2006). RCs also receive direct cholinergic input from motor neurons, whereas IaINs do not (Alvarez and Fyffe, 2007).

1.8 Presynaptic inhibitory interneurons and gain control

The sensory-motor reflex circuit is modulated by a number of different interneurons. From the point of view of the sensory-motor reflex circuit, there

are two GABAergic subtypes, those that form direct contacts onto motor neurons, and those that form axo-axonic contacts onto the sensory terminals that contact motor neurons (Frank and Fuortes, 1957; Mears and Frank, 1997; Rudomin, P. & Schmidt, 1999; Betley et al., 2009). These latter cells are termed GABApre neurons due to their direct contacts with sensory neuron terminals, the pre-synaptic neuron in the sensory-motor circuit (Hughes et al., 2005; Betley et al., 2009), and their expression of GABA. GABApre neurons mediate presynaptic inhibition, by attenuating transmitter release onto postsynaptic neurons. Presynaptic inhibition occurs throughout the CNS (Rudomin, 2009; Kubota et al., 2016). For example in the cortex, Chandelier cells are one type of cortical inhibitory interneuron that preferentially forms axo-axonic contacts onto the axon initial segment of pyramidal cells (Jiang et al., 2015; Kubota et al., 2016).

Presynaptic inhibition exerted by GABApre boutons on sensory terminals results in primary afferent depolarization (PAD), which causes motor neurons to be less likely to fire (Eccles et al., 1961, 1962, 1963). Pharmacological studies determined that GABA is the neurotransmitter mediating presynaptic inhibition (Eccles et al., 1963), and electron microscopy provided anatomical evidence of GABApre boutons on sensory afferent terminals (Conradi, 1969). Furthermore, presynaptic inhibition can be measured in living organisms by measuring the H-reflex, which is the reflex in muscles following electrical stimulation of sensory afferents (Knikou, 2008).

What is the function of GABApre neurons and presynaptic inhibition on sensory-motor drive? Recent work has shown that presynaptic inhibition is a way to modulate the gain of sensory neurons. Fink et al. (2014) found that

GABApre neurons are essential for mediating smooth movement of the forelimb. Ablating this cell subtype in mice and then subjecting these mice to a targeted reaching assay resulted in motor perturbations. Specifically, when GABApre-depleted mice attempted to reach for a pellet of food, their forelimb moved in an abnormal oscillatory motion and had difficulty grasping the pellet (Fig. 1.5). This suggests that GABApre neurons are essential for gating sensory gain during movement, and the absence of these cells results in gain overload and motor perturbations (Fink et al., 2014).

1.8.1 Molecular and cellular identity of GABApre neurons

GABApre neurons have been further characterized cellularly and molecularly. GABApre neurons express two specific GABA synthesizing enzymes, the glutamic acid decarboxylase (GAD) 67 as well as GAD65 (Hughes et al., 2005; Betley et al., 2009). GAD67 is localized cytoplasmically at the synapse, and is widely expressed in all GABAergic neurons in the spinal cord. GAD65 is vesicle bound at the synapse, and is largely restricted to GABApre neurons. Furthermore, GABApre boutons also express the synaptic-vesicle associated protein, Synaptotagmin 1 (Syt1). By using a combination of these GABApre synaptic markers, GABApre boutons can be visualized on sensory afferent terminals, which can be labeled with the vesicular glutamate transporter 1 (vGluT1) (Fig. 1.6). Moreover because GABApre neurons express *Ptf1a* during development, they can be permanently labeled using genetic lineage tracing with $Ptf1a^{Cre}$ mice intercrossed to a fluorescent reporter line. These data provide a toolbox with which to analyze GABApre boutons (Betley et al., 2009).

Figure 1.5: GABApre interneuron function

(A) Mice are tested for skilled forelimb movement, in which they reach for a pellet of food through a small opening.

(B) A virus for cre-recombinase dependent diphtheria toxin (DT) is injected into the spinal cord of *Gad2*^{Cre} mice, thereby killing *Gad2* expressing cells. GABApre boutons are maintained in mice before viral injection (Pre-DT), but mostly absent in *Gad2*^{Cre} mice after viral injection (Post-DT).

(C) Post-DT mice exhibit significant deficits in reaching for the pellet of food (red) when compared to Pre-DT mice (blue).

(D) Post-DT mice exhibit an abnormal oscillatory motion as their arms reach forward. Pre-DT mice reach in a smooth movement forward. These data suggest that GABApre neurons mediate smooth movement and gain control on sensory terminals. Adapted from Fink et. al, 2014.

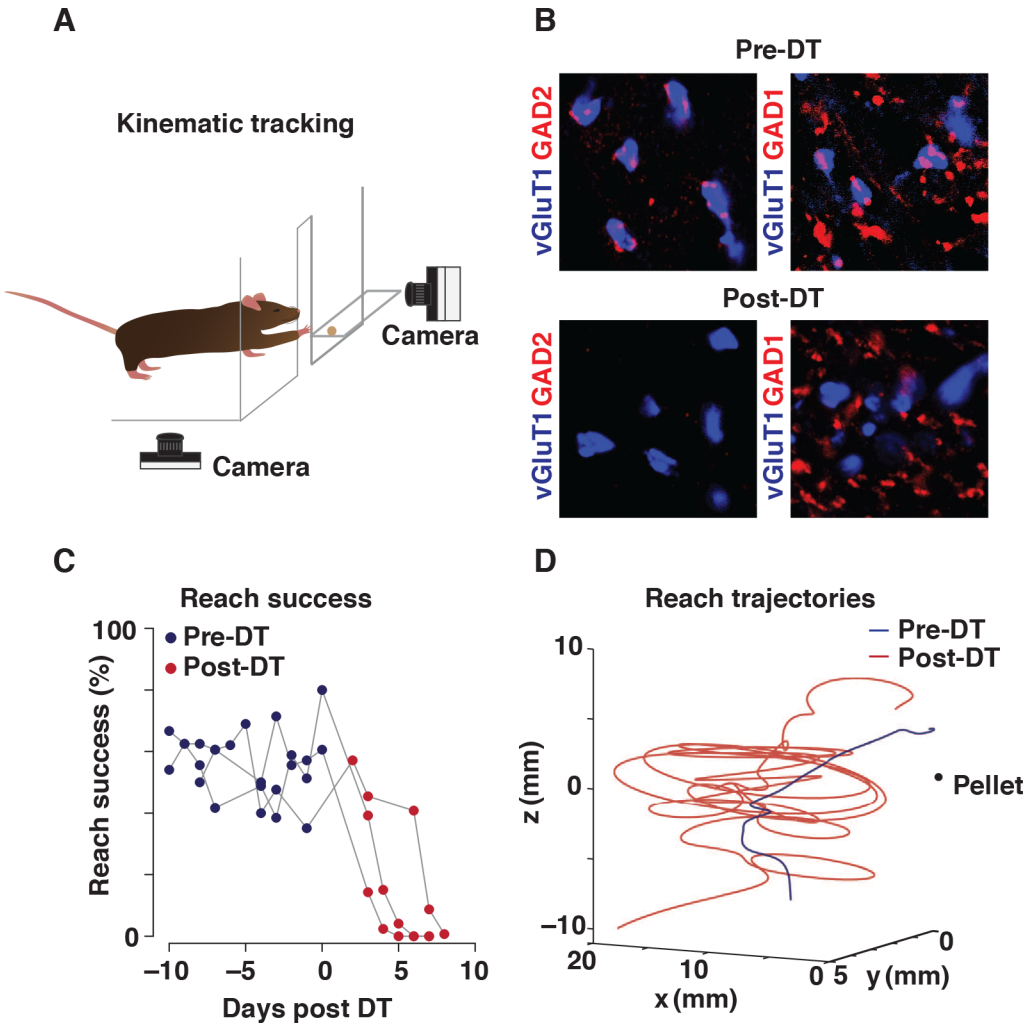
A
Kinematic tracking
Camera
Camera
B
Pre-DT
vGluT1 GAD2
vGluT1 GAD1
Post-DT
vGluT1 GAD2
vGluT1 GAD1
C
Reach success
Pre-DT
Post-DT
Reach success (%)
100
0
−10
−5
0
5
10
Days post DT
D
Reach trajectories
Pre-DT
Post-DT
Pellet
z (mm)
10
0
−10
20
10
0
x (mm)
0
5
y (mm)

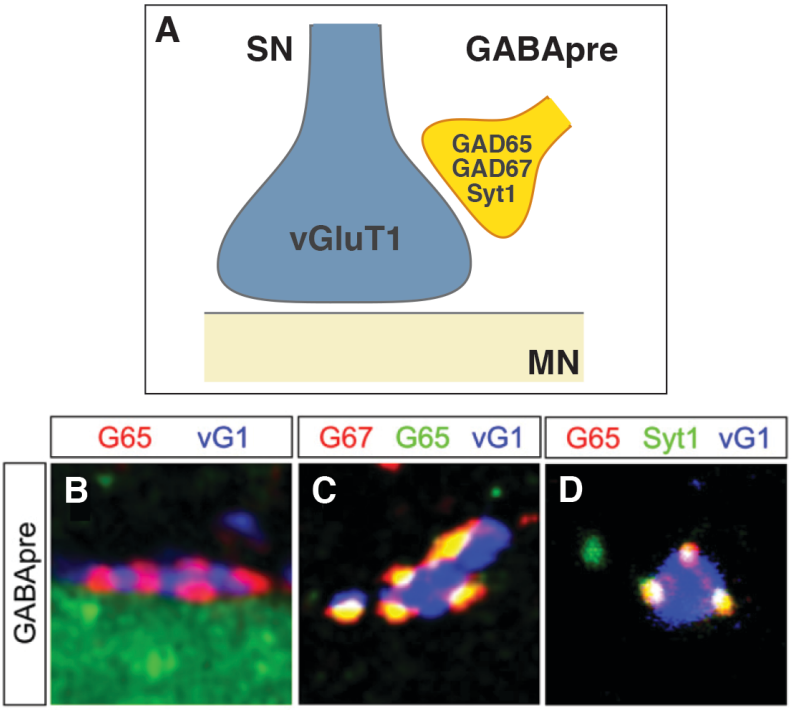

Figure 1.6: GABApre bouton molecular identification

(A) GABApre neurons can be colabeled with synaptic markers and form boutons on sensory neuron terminals (SN) that can be labeled with vGluT1, which contact motor neurons (MN).

(B-D) GABApre boutons can be labeled with GAD65 (G65), GAD67 (G67), and Syt1. Adapted from Betley et al., 2009.

There have been several lines of evidence suggesting that the neuronal source of GABApre neurons is in the intermediate spinal cord. Firstly, in a double fluorescent *in situ* hybridization experiment, Betley et al. (2009) observed overlap between *Gad1* (the gene for GAD67 expression) and *Gad2* (the gene for GAD65 expression) over a small region in the intermediate spinal cord. Since GABApre boutons uniquely express both GAD65 and GAD67, these neuronal cell bodies likely correspond to the GABApre population (Betley et al., 2009). Secondly, since GABApre projections extend to the ventral horn, retrograde labeling was used to trace the location of their cell bodies. Dextran, a tracer dye was injected by electrophoresis into the ventral horn of mice expressing GFP under the control of the GAD65 promoter ($GAD65^{GFP}$), resulting in a limited number of double-labeled, dextran/GFP double-positive cell bodies in the intermediate spinal cord (Hughes et al., 2005). Finally, electrophysiological data demonstrated that PAD could be specifically evoked during stimulation of the intermediate but not the dorsal spinal cord (Jankowska et al., 1981). Taken together, these three studies highly suggest that GABApre cell bodies reside in the intermediate spinal cord.

1.8.2 Synaptic specificity of GABApre neurons

GABApre boutons maintain a stringent specificity for their postsynaptic targets. When the sensory afferent synaptic target of GABApre neurons is absent, as in *Er81-/-* mouse mutants, GABApre neurons innervate the ventral spinal cord, but do not form synapses on any other possible synaptic targets in the ventral horn, and instead retract (Betley et al., 2009).

What mediates GABApre synaptic specificity? Since the only acceptable synaptic partner of GABApre boutons is sensory neurons, it would follow that a sensory-derived signal is responsible for GABApre synaptic specificity. Ashrafi et al. (2014) found that the immunoglobin (Ig) superfamily protein, contactin 5 (NB2) was co-expressed and interacted with the contactin-associated protein-like 4 (Caspr4) in proprioceptors. In the absence of one or both of these proteins in single and double mutant mice there was a 40% reduction in the number of GABApre boutons when compared to wild-type (wt) mice. While NB2/Caspr4 promotes GABApre bouton formation on the sensory neuron side, two members of the L1 Ig family, cell adhesion molecule L1-like (*CHL1*) and neuronal cell adhesion molecule (*NrCAM*) are also necessary on the GABApre neuron side. Loss of *CHL1* and *NrCAM* in GABApre neurons results in a loss of GABApre boutons on sensory afferent terminals. The interaction between sensory NB2/Caspr4 and interneuron NrCAM/CHL1 is an important, though not sole contributor to the formation of GABApre boutons on sensory terminals (Ashrafi et al., 2014a).

1.9 Motor diseases in humans involving presynaptic inhibition

In humans, deficits in presynaptic inhibition have been associated with several movement disorders such as dystonia, Huntington's disease, Parkinson's disease, and spasticity (caused by multiple sclerosis, stroke, spinal cord injury). By studying changes in the amplitude of the H-reflex in humans, potential deficits in presynaptic inhibition can be elucidated. The H-reflex is a measure of the excitability of motor neurons, which is usually measured in the forearm or leg of human subjects. Measuring the H-reflex

generates a curve that consists of two phases: the early phase that involves the reciprocal Ia inhibitory pathway due to postsynaptic mechanisms, and the late phase due to presynaptic inhibition. Differences in H-reflex amplitude following a conditioning stimulus can be used as a measure of the amount of presynaptic inhibition exerted on sensory afferent terminals. A larger H-reflex amplitude is a sign of decreased presynaptic inhibition (Fig. 1.7, Knikou, 2008).

Several motor diseases exhibit changes in the H-reflex that suggest a deficit in presynaptic inhibition. Both dystonia and Huntington's patients exhibited a larger H-reflex amplitude, and a significant change in the late phase of the H-reflex in upper limbs, signifying a deficit in presynaptic inhibition compared with normal subjects (Nakashima et al., 1989; Panizza et al., 1990; Priori et al., 2000).

In Parkinson's disease, major motor abnormalities exhibited by human patients are tremors, rigidity, and bradykinesia, which is a slowness of movement. Different groups have tested whether these symptoms could be tied to changes in presynaptic inhibition in lower limbs by measuring the H-reflex (Roberts et al., 1994; Morita et al., 2000). Measuring the H-reflex in the soleus muscle of human patients with Parkinson's disease showed deficits in presynaptic inhibition. There was no relation between decreased presynaptic inhibition and rigidity, but there was a relation between decreased presynaptic inhibition and slower walking speed and worsened bradykinesia (Roberts et al., 1994; Morita et al., 2000).

Finally, deficits in presynaptic inhibition as measured by changes in the H-reflex were also observed in patients suffering from spasticity, which can

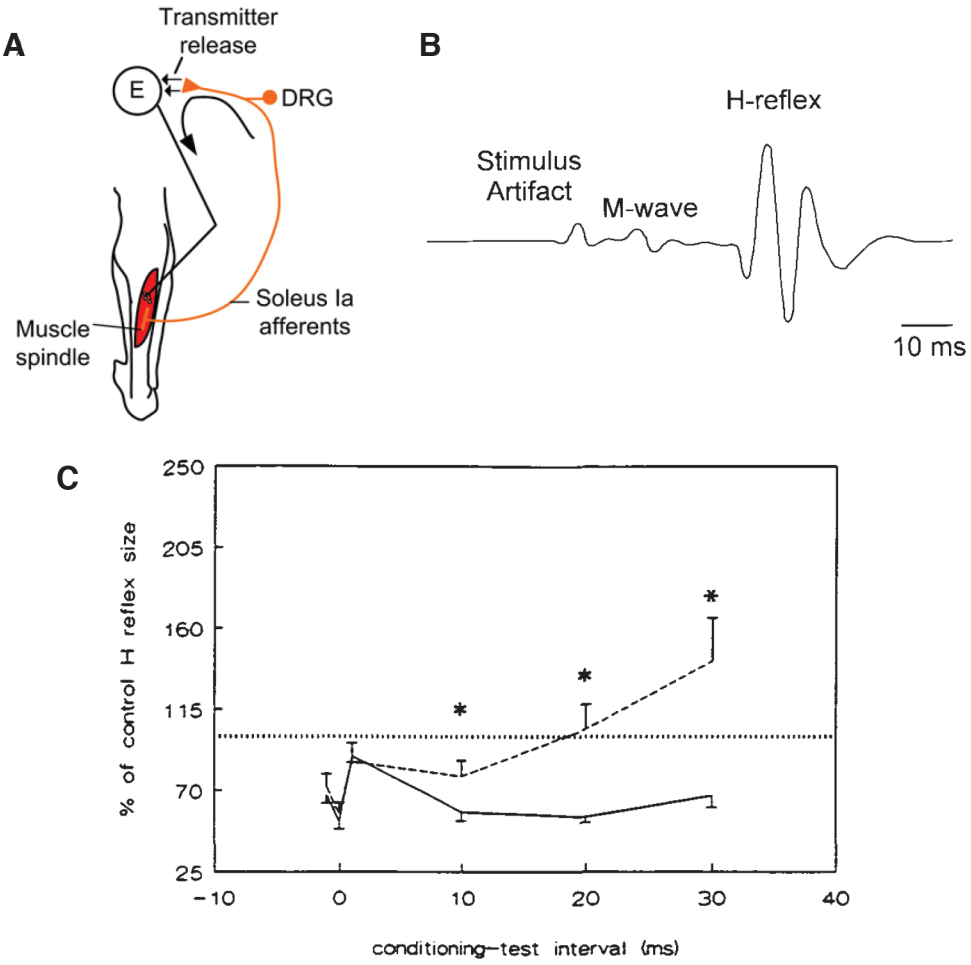

Figure 1.7: H-reflex as a measure of presynaptic inhibition

(A) The H-reflex measures the excitation of motor neurons, and can be used to measure changes of presynaptic inhibition in humans. The H-reflex can be measured from the soleus muscle upon conditioning stimuli applied to the nerve. From Knikou, 2008.

(B) Sample trace of electromyographic record of the H-reflex. From Misiaszek, 2003.

(C) There is a greater H-reflex size in human patients of dystonia when compared to normal humans, indicative of deficits in presynaptic inhibition on the sensory-motor circuit and greater activity in motor neurons. Presynaptic inhibition is measured from 10-20 ms. From Priori et al., 1995.

result from multiple sclerosis, stroke, or other insults to nervous tissue. Spasticity is characterized by continuous contraction in certain affected muscles and exaggerated jerks, caused by hyperexcitability of the stretch reflex (Morita et al., 2001). When compared to normal subjects, spastic multiple sclerosis patients have less presynaptic inhibition, which contributes to their inability to exert normal motor control (Morita et al., 2001).

1.9.1 Dystonia

Dystonia is a heterogeneous movement disorder characterized by involuntary sustained muscle contractions affecting one or more parts of the body. Dystonia is widely believed to reflect circuit dysfunction due to the absence of signs of neurodegeneration in the CNS of affected individuals. It is the third most common movement disorder in humans, and can be categorized as two types: primary and secondary dystonia. Primary dystonia develops spontaneously and is not caused by any previous insult to the body. In contrast, secondary dystonia results from an associated disease such as brain or spinal cord injury (Breakefield et al., 2008).

One type of primary dystonia is early-onset generalized dystonia, which begins to affect patients in childhood and early adolescence. Although the exact etiology of dystonia is not fully understood, there is a strong genetic link between early-onset generalized dystonia and genetic mutations. One mutation that is highly implicated in early-onset generalized dystonia is a mutation in the torsin family 1 protein (*Tor1a/Dyt1*). *Tor1a* encodes a protein in the adenosine triphosphate (ATP)-ase family that is involved in protein folding and trafficking (Breakefield et al., 2008; Charlesworth et al., 2013). Tor1a is

primarily localized to the lumen of the endoplasmic reticulum (ER) and the nuclear envelope (NE) (Goodchild et al., 2005; Granata et al., 2011).

Although *Tor1a* is expressed widely in several types of tissues, there is only a clinical manifestation of mutated Tor1a in neural tissue, suggesting that *Tor1a* plays a critical role in neurons (Granata et al., 2009). A common autosomal dominant mutation that is responsible for more than 50% of primary early-onset dystonia is a single glutamic acid deletion in Tor1a (Dyt1ΔE) (Ozelius et al., 1997). Several studies have been conducted to compare differences between wt Tor1a and the mutant Tor1a, Dyt1ΔE protein. An accumulation of Dyt1ΔE was found in multiple areas in the CNS between the NE layers in neurons, forming abnormal perinuclear membranous inclusions, which can alter the function of local proteins (Goodchild et al., 2005). Compared to wt Tor1a, Dyt1ΔE was unable to interact with itself or wt Tor1a, which is important since Tor1a has been found to form a multimeric complex in order to exert its enzymatic ATPase function catalyzing ATP into ADP *in vitro* (Pham et al., 2006). Furthermore, Dyt1ΔE showed decreased enzymatic function compared to wt protein, likely due to its inability to interact with itself (Konakova and Pulst, 2005).

Most of the work conducted on understanding dystonia has been focused on the brain. Since the Dyt1ΔE mutation is highly implicated in the development of dystonia in humans, several groups have recapitulated the same genetic mutation in mouse models of dystonia. Mice that are heterozygous for *Dyt1ΔE* are evaluated for behavior as well as molecular and cellular changes in the hippocampus, cortex, and cerebellum (Goodchild et al., 2005; Vanni et al., 2015; Yokoi et al., 2015). These mice exhibited motor

abnormalities that included hyperactivity and deficits in beam walking (Dang et al., 2005). They also had decreased frequency of spontaneous (s)EPSCs in hippocampal slices, suggesting presynaptic release deficits (Yokoi et al., 2013). The motor deficits and presynaptic release deficits observed in *Dyt1ΔE* mice are comparable to those seen in Tor1a knockdown and knockout (KO) animals, suggesting that the Dyt1ΔE mutation is a loss-of-function (Dang et al., 2006; Yokoi et al., 2015). More recently, mutant mice in which *Tor1a* is knocked out in cortical regions and the striatum exhibited dystonic behaviors more closely aligned with those observed in human dystonia patients. Specifically, these mutant mice exhibited trunk twisting and limb clasping (Liang et al., 2014; Pappas et al., 2015).

1.9.2 Tor1a and Klhl14 binding

How does mutant *Tor1a* result in dystonic behaviors? Besides being able to interact with itself, Tor1a also binds other proteins such as kelch-like family member 14 (Klhl14). Tor1a and Klhl14 are coexpressed in neural tissues, and colocalize in the ER. They bind as co-factors, and their binding is disrupted although not entirely abolished by the human Dyt1ΔE mutation (Giles et al., 2009). *Klhl14* expression is present in the intermediate spinal cord and is *Ptf1a* dependent (Wildner et al., 2013), which suggests that it may be expressed in GABApre neurons. Despite knowledge of Klhl14-Tor1a binding, the function of Klhl14 protein in spinal cord circuitry is completely unknown.

In the next part of my thesis work, I use genetic analysis and developmental timing to localize *Klhl14* expression in GABApre neurons, and

show defects in GABApre circuitry in mice carrying a genetic mutation that is linked to the motor disease, dystonia.

Chapter 2

Screen for specific GABAergic subgroups identifies role for Dystonia-associated genes in spinal circuitry

Authors: Juliet Zhang[1,2,6], Jarret A. P. Weinrich[1,3,6], Jeffery B. Russ[1,4], John D. Comer[1,4], Praveen K. Bommareddy[1], Richard J. DiCasoli[1], Yuqing Li[5] and Julia A. Kaltschmidt[1,2,3,7]

[1] Developmental Biology Program, Sloan Kettering Institute, New York, NY, 10065, USA

[2] Neuroscience Program,

[3] Cell and Developmental Biology Program, Weill Cornell Medical College, New York, NY, 10065, USA

[4] Weill Cornell/Rockefeller/Sloan-Kettering Tri-Institutional MD-PhD Program, New York, NY, 10065, USA

[5] Department of Neurology, College of Medicine, University of Florida, Gainesville, FL, 32610, USA

[6] Co-first authors

[7] **Correspondence Author**: Julia A. Kaltschmidt, Developmental Biology Program, Sloan Kettering Institute and Neuroscience and Cell & Developmental Biology Programs, Weill Cornell Medical College, New York, NY, 10065, USA, kaltschj@mskcc.org

Conflict of Interest: The authors declare no competing financial interests.

2.1 Author Contributions

JZ performed *Ptf1a* timing study, *Klhl14* expression analysis, and *Dyt1ΔE* mutant analysis. JAPW performed screen for intermediate enriched genes, and data analysis for *Dyt1ΔE* mutant analysis. JBR established paradigm for tamoxifen injections. JDC provided cell distribution data analysis. PKB and RJD provided technical assistance. YL generated Dyt1ΔE mice. JZ, JAPW and JK designed the study, interpreted results, and wrote the paper.

2.2 Acknowledgements

This work was supported by an MSTP grant from the National Institute of General Medical Sciences of the NIH under award number T32GM007739 to the Weill Cornell/Rockefeller/Sloan-Kettering Tri-Institutional MD-PhD Program (JDC), NIH grants DK42502, DK089570, the Vanderbilt Center for Imaging Shared Resource, partly supported through the VUMC Digestive Disease Research Center, Diabetes Research Training Center, and Vanderbilt Ingram Cancer Center, supported by NIH grants CA68485, DK20593, DK58404, DK59637 (CVEW), by NIH grant R01-NS083998, Memorial Sloan-Kettering start-up funds, a Whitehall Foundation Research Grant, a Louis V. Gerstner, Jr. Young Investigators Award and MSK Cancer Center Support Grant/Core Grant P30 CA008748 (JAK). We are grateful to C. Wright for *Ptf1a*^{Cre} mice, *Ptf1a*^{CreER} mice and Ptf1a antibodies. We also thank N. Betley for the RFP antibody, and H. Wildner and C. Birchmeier for the *Klhl14* clone. We thank T. Milner for advice and guidance with pump perfusions, A. Joyner for the tamoxifen protocol and advice, J. Belluardo for perfusion assistance

and advice, A. Tyagi for cell counts, and R. Khanin and the Sloan Kettering Genomics and Bioinformatics cores for screen analysis and statistics. We thank P. van Roessel for comments on the manuscript.

2.3 Abstract

Deficits in presynaptic inhibition have been observed in human motor diseases such as dystonia. In the spinal cord, a specific subset of dorsal inhibitory interneurons called GABApre neurons modulate sensory-motor connectivity, and exert presynaptic inhibition on proprioceptive sensory afferent terminals in the ventral horn. Genetic markers to identify GABApre neurons, and their potential contribution to motor disease are relatively unknown. In this study, we find the kelch-like family member 14 Klhl14, which is implicated in dystonia through its direct binding with Tor1a, to be a expressed in GABApre neurons. Our data uses the timeline of Ptf1a expression to localize Klhl14 to late Ptf1a-derived interneurons in the intermediate spinal cord, which are GABApre neurons. Furthermore, we demonstrate that in a mutant mouse in which Klhl14 and Tor1a binding is disrupted, there is a deficiency in the number of properly formed GABApre boutons. Our findings suggest a potential contribution of GABApre neurons to the deficits in presynaptic inhibition observed in dystonia.

2.4 Significance Statement

Neural circuitry dysfunction has been linked to human motor disorders such as dystonia, in which patients exhibit deficits in presynaptic inhibition. Presynaptic inhibition is essential for proper motor control, and is mediated by spinal inhibitory interneurons. The link between spinal interneurons and motor disease is not well studied. In this report, we identified kelch-like family member 14 (*Klhl14*) and its cofactor *Tor1a* to be expressed in GABApre neurons. Mutations in *Tor1a* have been previously linked to dystonia, and we observe GABApre circuit deficits in mice mutant for *Tor1a*. These data provide evidence that *Klhl14* and *Tor1a* expression in GABApre neurons is important for their synapse formation.

2.5 Introduction

The specific organization of neuronal circuits is critical for the generation of normal animal behavior and such organization depends inherently on the precise differentiation and connectivity of component neurons. GABAergic inhibitory interneurons play crucial roles in neuronal circuits, modulating the excitability or output of nearby neurons in complex ways determined by their specific connectivity. In humans, dysfunction of inhibitory interneurons is thought to underlie the symptoms of diverse disorders such as spinal cord injury and cerebral palsy (Tillakaratne et al., 2000; Achache et al., 2010), which may in turn affect locomotor symptoms associated with these conditions, such as motor deficit, spasticity, and impaired voluntary movement (Comi et al., 2005; Achache et al., 2010). Yet

while injury or disease-related functional deficits have been identified in physiologically-defined spinal circuits, little is known about the potential involvement in these conditions of specific, molecularly-defined classes of inhibitory spinal interneurons.

A main circuit of movement control affected in locomotor disorders is the monosynaptic stretch reflex circuit, which can be assessed via the human H-reflex (Knikou, 2008). In this circuit, input from a peripheral muscle is relayed via proprioceptive sensory neuron afferents onto spinal motor neurons, which transmit the signal back to the muscle of origin (Eccles et al., 1957; Mears and Frank, 1997). Activity across this synapse is presynaptically modulated by a specific class of GABAergic interneurons, called GABApre neurons, which form presynaptic, axo-axonic synapses on sensory afferent terminals (Windhorst, 1996; Rudomin, P. & Schmidt, 1999; Betley et al., 2009). In our prior work (Betley et al., 2009) we identified and molecularly characterized GABApre interneurons. We demonstrated that they express Pancreas transcription factor *(Ptf) 1a*, and that their terminals can be visualized with both GABA synthetic enzymes GAD65 and GAD67, as well as the Ca^{2+} sensor Synaptotagmin-1 (Syt1), thus differentiating GABApre neurons from other Ptf1a-derived interneurons (Betley et al., 2009). Several lines of evidence have suggested GABApre cell bodies to reside in the intermediate spinal cord: *GAD65* and *GAD67* co-express in neuronal cell bodies of the intermediate spinal cord (Betley et al., 2009); injection of a tracer dye into the ventral motor column to which GABApre neurons project labels GAD65-expressing cell bodies in the intermediate spinal cord (Hughes et al., 2005); and electrical stimulation of the intermediate spinal cord leads to

primary afferent depolarization (PAD), considered to be a result of presynaptic inhibition (Jankowska et al., 1981).

Despite our knowledge of the afferent connectivity and molecular profile of GABApre interneurons, we know relatively little about the molecular strategies used to establish and maintain the specific connections between GABApre interneurons and their sensory afferent terminal targets. We further know little about what role the GABApre-sensory microcircuit may play in disease states, and whether changes in this circuitry may reflect causes of, or adaptations to, motor illnesses. Clues to the involvement of GABApre interneurons in such illnesses come from physiologic studies showing deficits in presynaptic inhibition in people affected by motor diseases. Individuals with dystonia, Huntington's disease, and Parkinson's disease show larger H-reflexes in upper limbs, signifying a deficit in presynaptic inhibition (Nakashima et al., 1989; Panizza et al., 1990; Roberts et al., 1994; Priori et al., 1995, 2000; Morita et al., 2000). However, the specific functional involvement of presynaptic inhibitory interneurons in these motor diseases is unknown.

In this study we used microarray and *in silico* screening techniques to identify a set of transcripts specifically expressed by inhibitory interneurons in the intermediate spinal cord. We identified *Klhl14* to be expressed in *Ptf1a*-derived cells, and used the timeline of *Ptf1a* expression to localize *Klhl14* expression to GABApre cell bodies in the intermediate spinal cord. To explore the consequences of disrupting *Klhl14* activity in GABApre interneurons, we used a mutant mouse (*Dyt1ΔE*) in which the binding partner of *Klhl14*, the more broadly expressed *Tor1a*, is mutated, resulting in a decrease in Klhl14 and Tor1a binding (Giles et al., 2009). Analysis of *Dyt1ΔE* mice showed a

decrease in GABApre bouton number on sensory afferent terminals, suggesting that *Klhl14* and *Tor1a* play a role in GABApre bouton formation. Taken together, our findings help define the organization and genetic profile of a discrete set of intermediate spinal inhibitory interneurons that exert significant modulatory action during motor behavior. Our results suggest a link between a genetic lesion and specific circuit level developmental and neurophysiological dysfunction.

2.6 Materials and Methods

2.6.1 Mouse Strains

The following mouse strains were used in this study: *Dyt1ΔE* (Dang et al., 2005), *Gad65::^{N45}GFP* (Lopez-Bendito et al., 2004), *Ptf1a^{Cre}* (Kawaguchi et al., 2002), *Ptf1a^{CreER}* (Pan et al., 2013), *R26$^{CAG-lox-STOP-tdTomato/+}$* (Jackson, Ai14) (Madisen et al., 2010), and *Thy1$^{lox-STOP-YFP}$* (line 15) (Buffelli et al., 2003). Experiments conform to the regulatory standards of the Institutional Animal Care and Use Committee of Memorial Sloan Kettering Cancer Center.

2.6.2 Tamoxifen Injections

Tamoxifen (TM) (T-5648; Sigma-Aldrich) was dissolved in corn oil (C-8267; Sigma-Aldrich) at a final concentration of 20 mg/ml. TM was intraperitoneally injected once into pregnant dams at 9.5 or 12.5 post-coitus, and pups were harvested at embryonic day (e)18.5 or postnatal day (p)21. For embryo harvest, 80-100 mg/kg TM was administered at both time points. For postnatal harvest, 20 mg/kg TM was administered at e9.5, and 100 mg/kg TM was administered at e12.5.

2.6.3 Histochemistry

Immunohistochemistry and *in situ* hybridization on 12 µm or 20 µm thick cryostat sections were performed as previously described (Arber et al., 1999; Betley et al., 2009) with the following modification: mice were perfused by peristaltic pump (World Precision Instruments) with a 2% heparin (Butler-Schein) normal saline solution flush, followed by room temperature 4% PFA.

Antibodies were used in 0.3% Triton-X in phosphate buffer saline (PBS) with 1% bovine serum albumin (BSA) or 0.1% PBT with 1% BSA. The following antibodies were used in this study: rabbit anti-GAD65 (1:8000; Betley et al. 2009), mouse anti-GAD67 (1:10,000; Millipore), rabbit anti-GFP (1:1000; Invitrogen), rabbit anti-Ptf1a (1:5000; generously provided by C. Wright), guinea pig anti-RFP (1:2000; generously provided by N. Betley; Betley et al., 2013), rabbit anti-RFP (1:1000; Rockland), rabbit anti-Shank1a (1:1000; Millipore), rabbit anti-Tor1a (1:600; Millipore), guinea pig anti-vGluT1 (1:32,000; Betley et al. 2009), and fluorophore-conjugated secondary antibodies (Jackson Labs and Molecular Probes).

In situ hybridization combined with antibody staining was performed as described (Ashrafi et al., 2014b). tdTomato or GFP detection in combination with *in situ* hybridization was performed with additional TSA amplification (Perkin-Elmer) of the RFP or GFP antibodies with donkey anti-rabbit HRP-conjugated secondary (1:1000; Millipore). *In situ* hybridization of *Gad1* (Russ et al., 2015), *Gad2* (Russ et al., 2015), and *Klhl14* (generously provided by H. Wildner and C. Birchmeier, Wildner et al. 2013), was performed with DIG-labeled riboprobes.

2.6.4 Synaptic Quantification

Synaptic number counts were performed using Leica LASAF software plug-in (Version 2.6.0.7266) on z stacks (0.3 µm optical sections) obtained on a Leica TCS SP5 confocal. At least three mice per genotype were analyzed and ≥ 100 vGluT1^{ON} sensory terminals were counted per animal. Differences between wild type and mutant mice were determined using t-test or two-way ANOVA. $p > 0.05$ n.s., $p < 0.01$ **, $p < 0.0001$ ****. Data are reported as mean ± SEM.

2.6.5 Candidate Screen

Spinal cords were removed from three p6 *Gad65::^{N45}GFP* mice, embedded in UltraPure L.M.P. agarose (Invitrogen) and vibratome sectioned at 300 µm. The dorsal, intermediate and ventral regions were then dissected from each section and flash frozen on dry ice. RNA was obtained by trizol extraction and run on an Alumina microarray. Gene expression data was analyzed using BioConductor suit of tools (www.bioconductor.org) in R statistical language (www.r-project.org). The data were normalized using standard gcrma function. For each group comparison, differentially expressed genes were sought using limma package with a p-value cut-off of 0.05 (adjusted for multiple hypothesis testing) and fold-changes of 2. Pathway analysis was done using the functional annotation tool DAVID https://david.ncifcrf.gov/.

2.6.6 Statistics

Probability densities of tdTomato-positive (tdTomato^{ON}) cell body position were calculated in e18.5 *Ptf1a^{Cre}; R26^{tdTomato}* embryos following TM injection at e9.5 and e12.5. Positional coordinates of tdTomato^{ON} cell bodies

were obtained using software developed in the laboratory (Russ et al., 2013). The positional coordinates were then processed in R statistical language using the kde2d function from the MASS package. Further computation and graphical display was also performed in R. Student's t-test or ANOVA was used for synaptic quantifications.

2.7 Results

2.7.1 Screen for motor disease associated markers enriched in the intermediate spinal cord

Disruption of the H-reflex, which is the reflexive activation of muscles following electrical stimulation of sensory afferents, is a feature of a number of human movement disorders, including dystonia and Parkinson's disease (Nakashima et al., 1989; Panizza et al., 1990; Roberts et al., 1994; Priori et al., 1995, 2000; Morita et al., 2001). Given the role of presynaptic inhibition in modulating the H-reflex (Knikou, 2008), and the known function of spinal GABApre interneurons in presynaptically inhibiting proprioceptive sensory inputs (Betley et al., 2009; Fink et al., 2014), we sought to better characterize the molecular profile of GABApre interneurons with a specific focus on markers that are associated with motor disease.

Based on previous results suggesting GABApre neurons reside in the intermediate spinal cord (Jankowska et al., 1981; Hughes et al., 2005; Betley et al., 2009), we performed a cDNA microarray screen comparing cDNA probes from intermediate spinal cord (I) with those from superficial dorsal (D) and ventral (V) domains of p6 *Gad65::*^{N45}*GFP* lumbar spinal cord, using GFP

expression as a visual marker of dorsal and intermediate domains (Fig. 1*A*). We found 268 genes to be differentially expressed in the intermediate spinal cord, of which 61 were greater than two-fold upregulated in the intermediate spinal cord compared to both the dorsal and ventral spinal cord (Fig. 1*A*). This subset encodes proteins with diverse molecular functions including DNA binding, ion binding, nucleotide binding, receptors, as well as those with unknown function (Fig. 1*B*).

For this list of 61 genes, we assessed the *in situ* spinal expression patterns in p4 mice *in silico* Allen Brain Atlas (http://www.brain-map.org/). We found 11 candidates to be exclusively expressed in the intermediate spinal cord (Fig. 1*C*). One of these genes was the kelch-like family member protein *Klhl14*, implicated in motor disease due to its direct binding of the dystonia 1 protein *Tor1a* (Giles et al., 2009). *Tor1a* encodes a protein in the ATP-ase family that is involved in protein folding and trafficking (Breakefield et al., 2008; Charlesworth et al., 2013). A single amino acid mutation in Tor1a, Dyt1ΔE, is highly implicated in early-onset generalized dystonia (Ozelius et al., 1997).

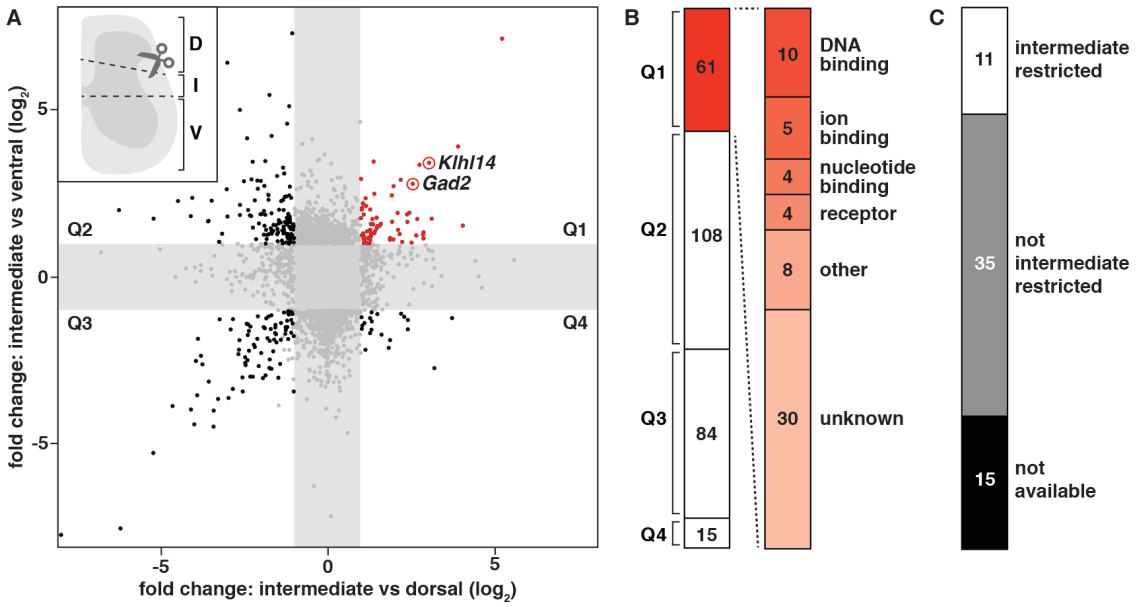

Figure 2.1: Screen for novel genes expressed in the intermediate spinal cord

(A) To find genes enriched in the intermediate spinal cord, gene expression levels were compared between dissected dorsal (D), intermediate (I) and ventral (V) spinal cord regions at p6 (see inset). Genes with significant ($p < 0.05$) and two fold or greater expression changes (268 genes) are graphed as a scatter plot comparing intermediate versus ventral (y-axis) and intermediate versus dorsal (x-axis) spinal regions. Genes that are upregulated in the intermediate region in both comparisons are in quadrant 1 (Q1, red, 61 genes), genes that are differentially expressed in both comparisons are in quadrant 2, 3, and 4 (Q2, 3, 4, black, 207 genes), and genes that are differentially expressed in either comparison are grey (1720 genes). Both *Gad2* and *Klhl14* are upregulated in the intermediate region (Q1).

(B) Functional classification of the 61 genes upregulated in both comparisons identified 4 main groups and many of unknown function.

(C) Analyzing *in situ* hybridization data from the Allen Brain Institute further restricted the 61 candidates to 11 genes (including *Klhl14*) that showed specific expression in the intermediate spinal cord.

2.7.2 *Klhl14* is expressed in intermediate inhibitory interneurons

Klhl14 has previously been shown to be expressed in the intermediate spinal cord (Wildner et al., 2013). We assessed the expression pattern of *Klhl14* more specifically using *in situ* hybridization. At late embryonic e18.5 (Fig. 2*A*) and early postnatal ages p5 and p10 (Fig. 2*B, C*), *Klhl14* was expressed in a restricted domain of the intermediate spinal cord, close to the central canal. This restricted expression pattern was maintained throughout the rostro-caudal extent of the lumbar spinal cord (Fig. 2*D*, red arrow). We did not detect *Klhl14* signal in the dorsal root ganglion (DRG), suggesting that *Klhl14* is not expressed in sensory neurons (Fig. 2*D*, black arrow).

We next asked if *Klhl14* was expressed in GABAergic inhibitory interneurons. The transcription factor *Ptf1a* is required for GABAergic neurotransmitter fate, and in the absence of *Ptf1a*, the precursors of spinal GABAergic interneurons give rise to excitatory glutamatergic neurons instead (Glasgow et al., 2005). In *Ptf1a* mutant spinal cords ($Ptf1a^{Cre/Cre}$), we observed no spinal expression of *Klhl14* (Fig. 2*E*).

To test whether *Klhl14* is expressed in *Ptf1a*-derived GABAergic interneurons, we labeled *Ptf1a*-derived neurons by intercrossing a $Ptf1a^{Cre}$ driver line (Kawaguchi et al., 2002) with mice carrying a $Thy1^{YFP}$ fluorescent protein reporter line (Buffelli et al., 2003) and performed dual immunohistochemistry/*in situ* hybridization using antibodies against GFP and a *Klhl14* RNA probe. We found that *Klhl14* expression strongly overlapped with YFP-expressing *Ptf1a*-derived neurons in the intermediate spinal cord (Fig. 2*F*). Given the observed absence of *Klhl14* expression in *Ptf1a* mutants,

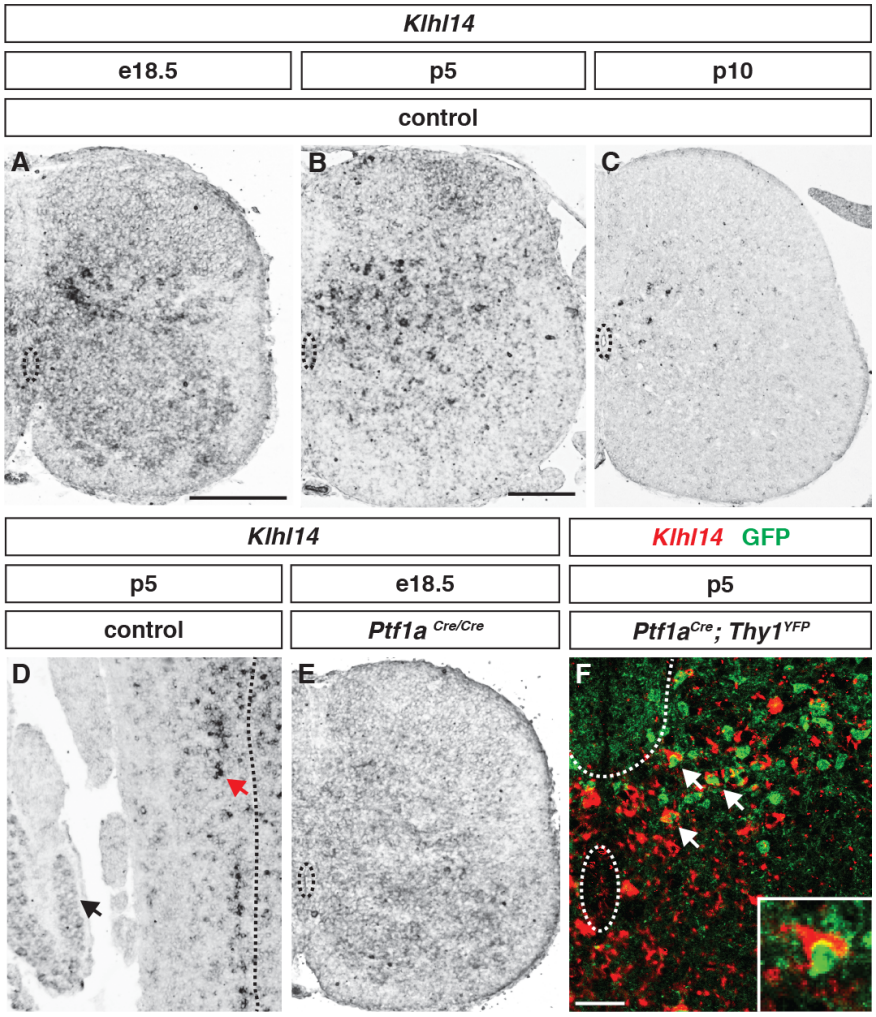

Figure 2.2: *Klhl14* expression in spinal inhibitory interneurons

(A-E) *Klhl14* transcript expression at e18.5 (A), p5 (B and D (red arrow)), and p10 (C). There is no *Klhl14* expression in DRG (D, (black arrow)). Dotted line in D depicts midline. *Klhl14* expression is absent in e18.5 Ptf1a mutant (*Ptf1a*$^{Cre/Cre}$) spinal cords (E).

(F) *Klhl14* transcript co-expression with fluorescently labeled GFP^{ON} (green) neurons in the intermediate spinal cord of *Ptf1a*^{Cre}*; Thy1*^{YFP} mice at p5. Scale bars: A, E, 200 µm; B-D, 100 µm; F, 50 µm.

we attribute the detection of *Klhl14* in neurons that are not YFP-expressing to the known mosaic expression of the *Thy1*^{YFP} allele (Betley et al., 2009). Taken together, these results suggest that *Klhl14* is specifically expressed in *Ptf1a*-derived interneurons of the intermediate spinal cord.

2.7.3 Late but not early Ptf1a expression distinguishes GABApre neurons

We next tested whether we could associate *Klhl14* labeling specifically with GABApre neurons, the subset of *Ptf1a*-derived GABAergic spinal interneurons that presynaptically inhibit sensory afferents (Hughes et al., 2005; Betley et al., 2009). Developmental timing can be harnessed as a tool to study subpopulations of cells (Tripodi et al., 2011; Benito-Gonzalez and Alvarez, 2012). To specifically correlate *Klh14* expression with GABApre neurons, we asked whether the GABApre neuron domain might be distinguished by specific timing of *Ptf1a* expression.

In the developing spinal cord, *Ptf1a* is expressed in postmitotic cells of the dI4/dILA precursor domain (Wildner et al., 2006). *Ptf1a* is expressed broadly in neuronal cell bodies throughout the dorsal-intermediate spinal cord between the time points of e9.5 and e13.5 (data not shown, Glasgow et al., 2005; Mizuguchi et al., 2006; Wildner et al., 2006). We first sought to recapitulate this broad dorsal expression by generating *Ptf1a*^{Cre} mice carrying a tdTomato(tdT)-reporter line (*R26*$^{CAG\text{-}lox\text{-}STOP\text{-}tdTomato}$) (Madisen et al., 2010) (Fig. 3*B*). We confirmed that this cross labels GABApre interneurons by assessing tdTomato expression in ventral axo-axonic synapses (Fig. 3*C*) that

Figure 2.3: *Klhl14* is expressed in GABApre neurons

(A) *Ptf1a* expression timeline and tamoxifen (TM) injection paradigm.

(B) tdTomato^{ON} (red) cells in the dorsal-intermediate spinal cord of *Ptf1a^{Cre}; R26^{tdTomato}* mice at e18.5.

(C) tdTomato^{ON} (red) boutons on vGluT1^{ON} (blue) sensory terminals in the ventral horn of p21 *Ptf1a^{Cre}; R26^{tdTomato}* mice.

(D, E) tdTomato^{ON} (red) boutons on vGluT1^{ON} (blue) sensory terminals co-express GABApre synaptic markers GAD65 (green, D) and GAD67 (green, E).

(F) tdTomato^{ON} (red) cells in the dorsal spinal cord of e9.5 TM injected *Ptf1a^{CreER}; R26^{tdTomato}* mice at e18.5.

(G-I) No ventral tdTomato^{ON} projections in e9.5 TM injected *Ptf1a^{Cre}; R26^{tdTomato}* mice at p21.

(J) tdTomato^{ON} (red) cells in the intermediate spinal cord of e12.5 TM injected *Ptf1a^{CreER}; R26^{tdTomato}* mice at e18.5.

(K-M) tdTomato^{ON} (red) boutons project into the ventral spinal cord (K) in e12.5 TM injected *Ptf1a^{Cre}; R26^{tdTomato}* mice at p21 and express GABApre synaptic markers GAD65 (green, L) and GAD67 (green, M).

(N) At e18.5, *Gad2* (blue) expressing *Ptf1a*-derived cells in e12.5 TM injected *Ptf1a^{CreER}; R26^{tdTomato}* mice settle in the intermediate spinal cord (n = 159, three mice).

(O) At e18.5, *Klhl14* (red) expressing *Ptf1a*-derived cells in e12.5 TM injected *Ptf1a^{CreER}; R26^{tdTomato}* mice settle in the intermediate spinal cord (n = 183, three mice).

(P) Overlay of *Gad2* (blue) and *Klhl14* (red) expression patterns in late *Ptf1a*-derived cells. Scale bars: B, F, J, 50 µm; C-E, G-I, K-M, 2 µm.

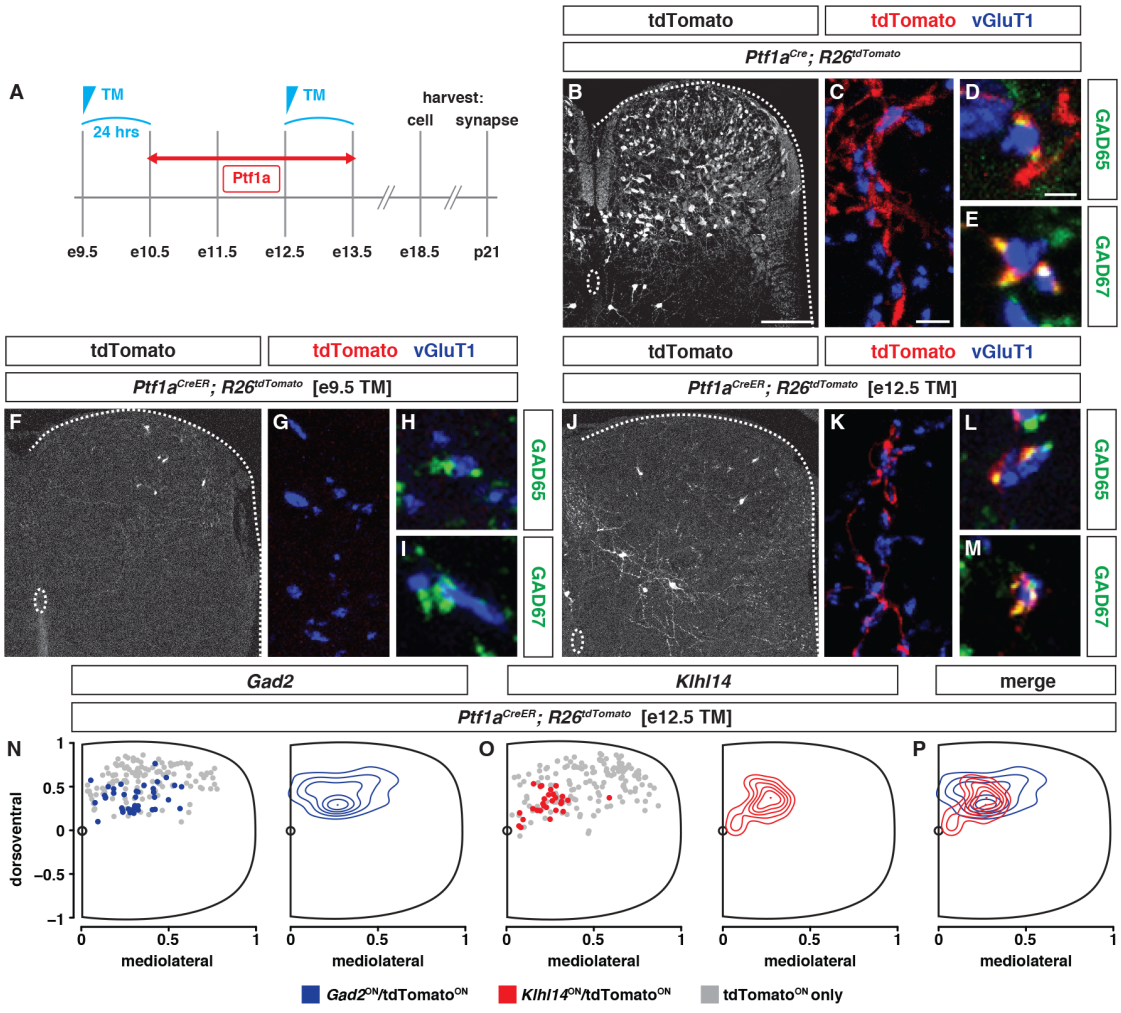
A
TM
24 hrs
TM
harvest:
cell
synapse
Ptf1a
e9.5
e10.5
e11.5
e12.5
e13.5
e18.5
p21
tdTomato
tdTomato vGluT1
Ptf1a^Cre; R26^tdTomato
B
C
D
E
GAD65
GAD67
tdTomato
tdTomato vGluT1
Ptf1a^CreER; R26^tdTomato [e9.5 TM]
F
G
H
I
tdTomato
tdTomato vGluT1
Ptf1a^CreER; R26^tdTomato [e12.5 TM]
J
K
L
M
GAD65
GAD67
Gad2
Klhl14
merge
Ptf1a^CreER; R26^tdTomato [e12.5 TM]
N
O
P
dorsoventral
mediolateral
Gad2^ON/tdTomato^ON
Klhl14^ON/tdTomato^ON
tdTomato^ON only

abut vGluT1-expressing sensory terminals. We further show that these tdTomato-expressing synapses on vGluT1 sensory terminals express the GABA-synthetic enzyme GAD65 and GAD67, known markers of GABApre boutons (Hughes et al., 2005; Betley et al., 2009) (Fig. 3*D-E*).

We next assessed whether the timing of *Ptf1a* expression could be used to identify specific subpopulations of *Ptf1a*-derived interneurons. To accomplish this, we used an inducible *Ptf1a*^{CreER} mouse line (Pan et al., 2013) and injected tamoxifen (TM) at different time points (Nguyen et al., 2009) (Fig. 3*A*). We found that injecting 100 µg/g TM at e9.5 or e12.5 gave rise to fluorescently labeled *Ptf1a*-derived neurons in distinct domains of the dorsal and intermediate spinal cord (Fig. 3*F*, *J*). In all *Ptf1a*-derived cells, labeled neurons localized to both the dorsal and intermediate spinal cord (Fig. 3*B*). TM injection at e9.5 predominately labeled neurons localized to superficial layers of the dorsal horn (Fig. 3*F*), while TM injection at e12.5 predominantly labeled neurons localized to the intermediate spinal cord (Fig. 3*J*). This suggests that putative GABApre cell bodies in the intermediate spinal cord derive from relatively late *Ptf1a*-expressing precursors, and may be distinguished on this basis.

We next sought to confirm whether these putative GABApre cells are in fact GABApre interneurons. We asked whether tdTomato^{ON} terminals, labeled via e9.5 or e12.5 TM injections, form axo-axonic contacts on proprioceptive terminals in the ventral spinal cord and express typical GABApre markers. We found that neurons labeled at e9.5 TM did not project ventrally (Fig. 3*G-I*). In contrast, we found that neurons labeled at e12.5 TM did project ventrally, formed contacts on vGluT1^{ON} sensory terminals (Fig. 3*K*), and expressed the

GABApre specific markers GAD65 (Fig. 3*L*) and GAD67 (Fig. 3*M*). Thus, TM injections into *Ptf1a*^{CreER}; *R26*^{tdTomato} mice at e12.5 label GABApre interneurons.

2.7.4 Klhl14 is expressed in GABApre neurons

To determine whether *Klhl14* labels GABApre neurons, we performed TM injections at e9.5 and e12.5 into *Ptf1a*^{CreER}; *R26*^{tdTomato} mice and performed dual immunohistochemistry/*in situ* hybridization staining using anti-RFP antibody and a *Klhl14* RNA probe. We found that in e12.5 TM injected mice tdTomato^{ON} cells in the intermediate spinal cord co-express *Klhl14* (Fig. 3*O*). We performed analogous immunohistochemistry/*in situ* labeling for RFP and *GAD2* transcript, the primary molecular marker for GABApre neurons, and similarly saw strong colocalization (Fig. 3*N*). In these experiments, the domains of coexpression of *Klhl14* and tdTomato and *GAD2* and tdTomato were highly similar (Fig. 3*P*), confirming the strong correlation of their expression in GABApre neurons.

2.7.5 GABApre bouton formation is disrupted in *Tor1a* mutant mice

We next assessed whether *Klhl14* has a functional role of in GABApre neurons. Little is known about the function of *Klhl14*, other than that it is a cofactor of the dystonia 1 protein Tor1a, which it binds in the endoplasmic reticulum of neurons (Giles et al., 2009). Deletion of a single glutamic acid residue in the C-terminal region of Tor1a (ΔE) severely disrupts binding to Klhl14 (Ozelius et al., 1997; Giles et al., 2009), and in humans, this mutation

causes early-onset generalized torsion dystonia, characterized by sustained muscle contractions involving both agonist and antagonist muscles (Ozelius et al., 1997; Breakefield et al., 2008). We assessed the spinal expression of *Tor1a* in mouse and found that it was expressed in proprioceptive sensory neurons in the DRG (data not shown), as well as in the spinal cord, including the majority of *Ptf1a*-derived interneurons in the intermediate spinal cord (Fig. 4*A, B*). These data confirm that both *Klhl14* and its binding partner *Tor1a* are expressed in *Ptf1a*-derived inhibitory interneurons in the intermediate spinal cord.

Given the localization of *Klhl14* and *Tor1a* to putative GABApre neurons, and given that individuals with dystonia often show deficits in the proprioceptive-mediated H-reflex (Nakashima et al., 1989; Panizza et al., 1990; Priori et al., 1995), we sought to assess the function of Klhl14-Tor1a binding in GABApre interneuron circuitry. To do this, we used *Dyt1ΔE* mice (Dang et al., 2005), which have a single amino acid deletion in Tor1a that mirrors the human mutation and disrupts Tor1a binding to Klhl14. We used male mice heterozygous for the mutant allele, which are viable and display motor abnormalities such as deficits in beam walking and hyperactivity at six months of age (Dang et al., 2005).

Dyt1ΔE mice have been shown to have deficits in synaptic vesicle recycling and synaptic protein stabilization in neural tissues such as the hippocampus and cerebellum (Kim et al., 2010; Granata et al., 2011). Because *Tor1a* is expressed in proprioceptive neurons of the DRG, we first assessed sensory-motor connectivity in *Dyt1ΔE* mice. We assessed proprioceptive

Figure 2.4: Abnormal GABApre synaptic organization in Dyt1ΔE mice

(A) tdTomato^{ON} (red) neurons in the intermediate spinal cord of *Ptf1a^{Cre}; R26^{tdTomato}* mice.

(B) Tor1a (green) expression in tdTomato^{ON} (red) neurons in *Ptf1a^{Cre}; R26^{tdTomato}* mice at p5.

(C) Schematic showing sensory neuron (SN) terminals express vGluT1 and are adjacent to Shank1a on motor neurons (MN). GABApre boutons express GAD65 and GAD67.

(D, E) vGluT1^{ON} (blue) sensory terminals are adjacent to Shank1a (red) in wt (D) and *Dyt1ΔE* mice (E) at p21.

(F, G) Sensory terminal density (F, wt: 1.18 ± 0.12, n = 570 terminals, three mice; *Dyt1ΔE*: 0.97 ± 0.18, n = 469 terminals, three mice; t-test, p = 0.4 n.s.) and volume (G, wt: 1.69 ± 0.1, n = 570 terminals, three mice; Dyt1ΔE: 1.46 ± 0.11, n = 469 terminals, three mice; t-test, p = 0.11 n.s.) are normal in *Dyt1ΔE* mutant mice compared to wt controls.

(H, I) tdTomato^{ON} (red) cells in *Ptf1a^{Cre}; R26^{tdTomato}* control (H) and *Ptf1a^{Cre}; R26^{tdTomato}; Dyt1ΔE* mice (I).

(J) The number of putative GABApre neurons is normal in *Dyt1ΔE* mice (wt: 24.5 ± 1.4, three mice; *Dyt1ΔE*: 25.4 ± 1, three mice; t-test, p = 0.66 n.s.)

(K-M) Fewer GAD65^{ON} (green)/GAD67^{ON} (red) GABApre boutons (yellow) on vGluT1^{ON} (blue) sensory terminals in p21 *Dyt1ΔE* mutant mice (L, L') compared to wt mice (K, K'). Compiled average number of GAD65^{ON}/GAD67^{ON} GABApre boutons on vGluT1^{ON} sensory terminals is reduced by 20% in *Dyt1ΔE* mutant mice (M, wt: 2.30 ± 0.11, n = 335 terminals, three mice; *Dyt1ΔE*: 1.87 ± 0.1, n = 304 terminals, three mice; ANOVA, $p < 0.01$ **).

(N-P) Fewer GAD65^{ON} (green)/GAD67^{ON} (red) GABApre boutons (yellow) on vGluT1^{ON} (blue) sensory terminals in 6 month old *Dyt1ΔE* mutant mice (O, O') compared to wt mice (N, N'). Compiled average number of GAD65^{ON}/GAD67^{ON} GABApre boutons on vGluT1^{ON} sensory terminals is reduced by 26% in *Dyt1ΔE* mutant mice (P, wt: 2.49 ± 0.12, n = 344 terminals, three mice; *Dyt1ΔE*: 1.82 ± 0.1, n = 330 terminals, three mice; ANOVA, $p < 0.0001$ ****). Scale bars: A, B, 50 µm; D, E, K-O', 2 µm; H, I, 200 µm.

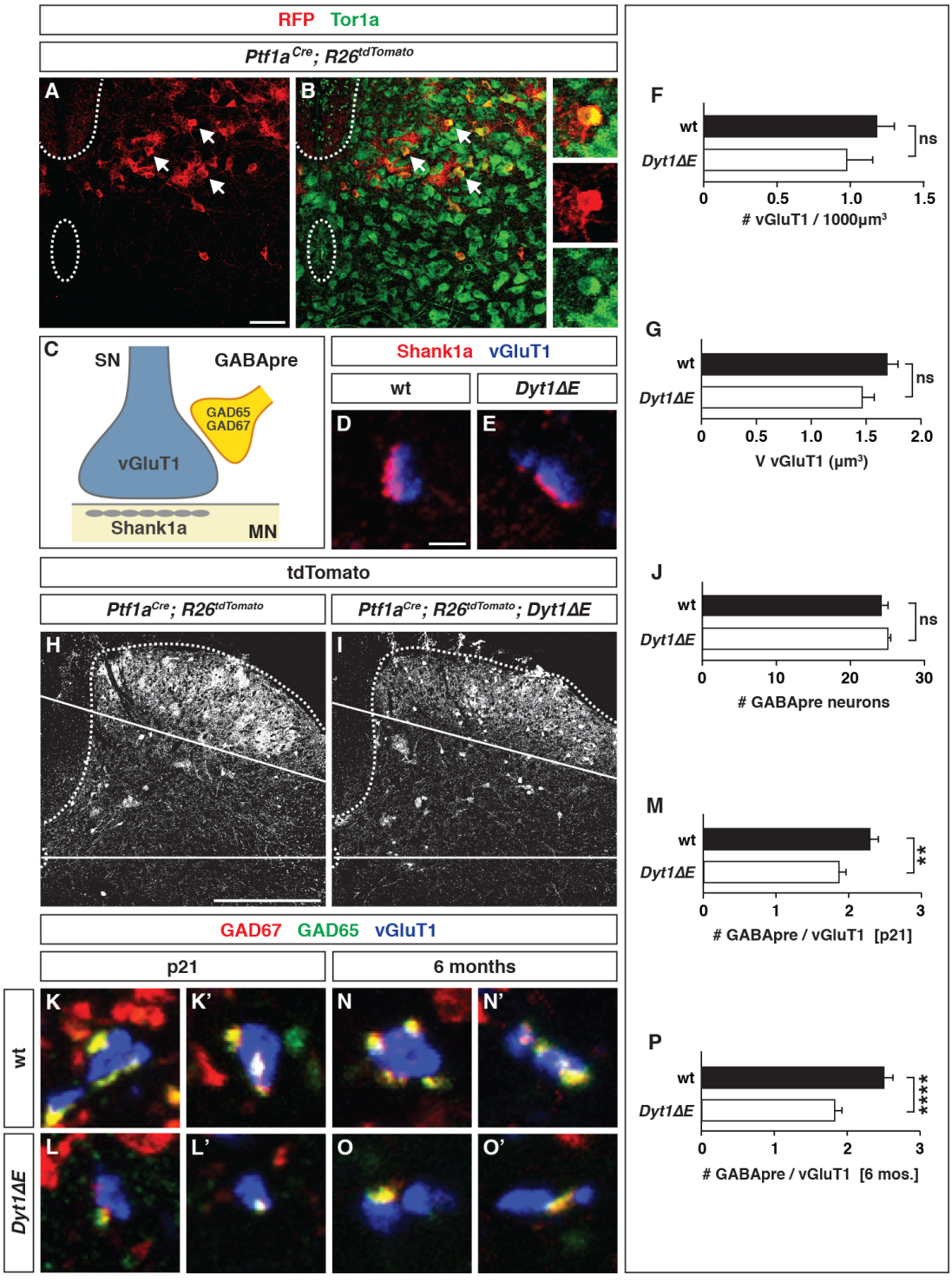
RFP Tor1a
Ptf1a Cre; R26 tdTomato
A
B
C
SN
GABApre
GAD65
GAD67
vGluT1
Shank1a
MN
Shank1a vGluT1
wt
Dyt1ΔE
D
E
tdTomato
Ptf1a Cre; R26 tdTomato
Ptf1a Cre; R26 tdTomato; Dyt1ΔE
H
I
GAD67 GAD65 vGluT1
p21
6 months
wt
Dyt1ΔE
K
K'
N
N'
L
L'
O
O'
F
wt
Dyt1ΔE
ns
0 0.5 1.0 1.5
vGluT1 / 1000µm3
G
wt
Dyt1ΔE
ns
0 0.5 1.0 1.5 2.0
V vGluT1 (µm3)
J
wt
Dyt1ΔE
ns
0 10 20 30
GABApre neurons
M
wt
Dyt1ΔE
**
0 1 2 3
GABApre / vGluT1 [p21]
P
wt
Dyt1ΔE
****
0 1 2 3
GABApre / vGluT1 [6 mos.]

afferent terminal number and density on motor neurons to verify the normal differentiation of sensory-motor synapses. Using vGluT1 to label sensory terminals (Fig. 4*C*), we found that the vGluT1^{ON} sensory terminal number and density were comparable between wild type and *Dyt1ΔE* mice (Fig. 4*F, G*; p = 0.4 and p = 0.11). The alignment of post-synaptic density marker, Shank1a, with vGlut1^{ON} sensory terminals (Fig. 4*D, E*) was also unchanged. Thus, proprioceptive afferent terminals are normal in *Dyt1ΔE* mice as compared to wild type mice.

We next analyzed GABApre circuitry by first testing whether the number of GABApre neurons is altered in *Dyt1ΔE* mice. To label putative GABApre neurons, we intercrossed the *Dyt1ΔE* mice with *Ptf1a*^{Cre}; *R26*^{tdTomato} mice, and assessed whether the number of GABApre neurons remains the same (Fig. 4*H, I*). We saw no difference in the number of tdTomato^{ON} putative GABApre neurons in the intermediate region in *Dyt1ΔE* compared to wild type mice (Fig. 4*J*; p = 0.66). We next assessed whether GABApre synaptic organization was affected in *Dyt1ΔE* mice. We used the co-expression of the two GABApre bouton markers, GAD65 and GAD67 (GAD65^{ON}/GAD67^{ON}) on vGluT1^{ON} sensory terminals to label GABApre boutons (Fig. 4*C*). We quantified the number of GAD65^{ON}/GAD67^{ON} boutons at p21 when locomotor circuits have finished developing (Fig. 4*K-I'),* as well as at 6 months (Fig. 4*N-O'*) when a behavioral motor defect is first observed in *Dyt1ΔE* mice (Dang et al., 2005). We found a 20% and 26% reduction in the number of GAD65^{ON}/GAD67^{ON} boutons on vGluT1^{ON} sensory terminals in *Dyt1ΔE* mice as compared to wild type controls at p21 (Fig. 4*M*; ANOVA, $p < 0.01$ **) and 6 months, respectively (Fig. 4*P*; ANOVA, $p < 0.0001$ ****). We observed no increase of either

GAD65^{ON} or GAD67^{ON} boutons, suggesting there is a joint loss of both markers (data not shown). These findings suggest that Klhl14-Tor1a binding in GABApre interneurons is required for normal GABApre-sensory terminal formation.

2.8 Discussion

Spinal interneurons are essential for modulating locomotor behavior, but their potential involvement in many motor disease states is unclear. Deficits in presynaptic inhibition of proprioceptive sensory afferents have been observed in human patients with movement disorders or focal motor deficits (Nakashima et al., 1989; Panizza et al., 1990; Priori et al., 2000), however, suggesting a potential role for GABApre interneurons in the pathophysiology of such disorders.

In this work, we demonstrate that despite the remarkable diversity of interneuron subtypes in the central nervous system, an approach using knowledge of molecular markers combined with developmental lineage analysis can be used to isolate and identify specific subclasses of spinal interneurons. Thus identified, further transcriptional screening approaches can identify new subclass-specific molecular markers that can begin to relate specific neuronal microcircuits to genetic disorders of nervous system functioning. As proof of this principle, we have identified the kelch-like family member protein *Klhl14* as specifically expressed in spinal GABApre interneurons, and show that mutation of a hereditary dystonia-related gene,

the Klhl14 binding partner Tor1a, at a site that disrupts binding to Klhl14, leads to measurable deficits in GABApre-sensory neuron connectivity.

2.8.1 Molecular characterization and transcriptional screening of GABApre neurons

Ptf1a is expressed in postmitotic cells of the dI4/dILA precursor domain (Wildner et al., 2006). In our prior published work (Betley et al., 2009), we characterized synapses deriving from *Ptf1a*-expressing (Ptf1a^{ON}) interneurons and inferred two different interneuron populations: (i) one that forms direct axo-axonic connections with proprioceptive sensory terminals in the intermediate and ventral spinal cord (GABApre) (Hughes et al., 2005; Betley et al., 2009) and (ii) one that forms axo-axonic contacts in the dorsal spinal cord. We further showed that the interneuronal synapses formed dorsally can be distinguished from those in the intermediate and ventral spinal cord in that the dorsal terminals are peptidergic and express the glycine transporter (GlyT)2, while the ventral GABApre boutons are neither glycinergic nor peptidergic, and express GAD65, GAD67 and Syt1 (Betley et al., 2009). Our molecular anatomic work thus supports the long standing hypothesis based on electrophysiological evidence that a dorsal interneuron population presynaptically inhibits cutaneous sensory terminals in the dorsal spinal cord, while an intermediate population projects ventrally and contacts proprioceptive sensory terminals in the intermediate and ventral spinal cord (Jankowska et al., 1981).

In this work, we confirm that the cell bodies of ventrally projecting GABApre interneurons are located in the intermediate spinal cord, and further demonstrate that their segregation to this region reflects specific developmental timing. In the spinal cord, interneuronal diversification begins embryonically with discrete progenitor domains giving rise to specific cell populations. One progenitor domain, known as dI4 during a first wave of neurogenesis, and dILA during a second wave of neurogenesis, gives rise to all *Ptf1a*-derived dorsal inhibitory interneurons, including GABApre neurons. Our molecular labeling and developmental timing studies identify the specific GABApre subclass of dorsal inhibitory interneurons as selectively localized to the intermediate spinal cord and emerging from dILA during the second wave of neurogenesis. This suggests a strong correlation between developmental timing, cell position and target selection and supports previous findings that showed premotor interneuron segregate by timing of neurogenesis (Tripodi et al., 2011).

2.8.2 Tor1a function in GABApre circuitry

Tor1a has been shown to play a role at synapses in synaptic vesicle recycling (Granata et al., 2008, 2011). In mouse cerebellum, there is a decrease in inhibitory synaptic contacts on Purkinje cells in both *Tor1a+/-* mice and mice carrying the human *Dyt1ΔE* mutation, suggesting that GABAergic synaptogenesis is compromised in the presence of mutant Tor1a (Sharma, 2005; Vanni et al., 2015). Our study further supports a neurodevelopmental role for *Tor1a* in synaptogenesis. In mouse spinal cord, we find that GABApre

bouton formation is compromised in *Dyt1ΔE* mice, in that there is a decrease in GABApre contacts on sensory terminals.

2.8.3 Where is Tor1a functioning to affect GABApre synaptogenesis?

Human studies postulate that observed deficits in H-reflex are due to affected descending control of spinal circuitry. Specifically, basal ganglia dysfunction has been associated with symptoms of dystonia (Breakefield et al., 2008; Pappas et al., 2015). While there is no direct input from the basal ganglia to the spinal cord, basal ganglia project to the cortex and corticospinal tract (CST) projections have been shown to directly contact putative GABApre neurons (Russ et al., 2013). *Tor1a* is expressed in the cortex (Shashidharan et al., 2000), however, it is unknown whether it is specifically expressed in CST neurons. If *Tor1a* is expressed in CST neurons, then mutated *Tor1a*, *Dyt1ΔE* may be causing aberrant CST input on GABApre cell bodies. Interestingly, in a mouse model of perinatal stroke in which there is a gross loss of descending CST inputs to GABApre cell bodies, GABApre GAD65 levels are decreased, while GABApre bouton number remains the same (Russ et al., 2013). This suggests against the possibility that the *Dyt1ΔE* mutation is affecting cortical circuits.

Although *Klhl14* is expressed in intermediate neurons of the dorsal spinal cord and not in sensory neurons of the DRG, *Tor1a* is expressed in the DRG and a subset of proprioceptive sensory neurons (data not shown). The GABApre-sensory synapse phenotype of *Dyt1ΔE* mice may thus reflect

dysfunction of *Tor1a* in sensory proprioceptors. We believe this is unlikely for two reasons: the first is that we observe no change in the number of synaptic contacts by sensory proprioceptors on motor neurons; the second is that the *Dyt1ΔE* mutation specifically affects binding of Klhl14 to Tor1a, and that Klhl14 is specifically expressed in GABApre interneurons. We thus interpret that the *Dyt1ΔE* GABApre-sensory synapse phenotype reflects cell-autonomous functioning of Tor1a in GABApre interneurons.

2.8.4 Tor1a in GABAergic synaptogenesis

How loss of Tor1a contributes to the decreased number of GABApre-sensory synapses remains an outstanding question. The *Dyt1ΔE* mutation's disruption of Tor1a to Klhl14 binding may provide clues. While little is known about *Klhl14*, several studies have focused on other members of the Kelch-like protein family members. Namely, Klhl1 has been identified as an actin-binding protein that is expressed in the axons and dendrites of neurons and glia in the nervous system, modulates voltage-gated calcium channels (Nemes et al., 2000), and regulates neurite and cellular process extension (Seng et al., 2006; Jiang et al., 2007). Knockdown of Klhl1 in rat hippocampal cultures results in decreased number of excitatory and inhibitory synapses (Perissinotti et al., 2015). The loss of synapses seen in *Dyt1ΔE* mice hints that *Klhl14* may have a similar role to *Klhl1*. The specific synaptic function of Tor1a may further reflect its association with Klhl14, and Tor1a thus may be considered to have a role at the interface of synaptic membrane recycling and local cytoskeletal dynamics. Given that the *Dyt1ΔE* phenotype of decreased GABApre-sensory

synapse number is strikingly similar to that seen following deletion of Ig-superfamily adhesion molecules expressed in GABApre interneurons or their sensory afferent partners (Ashrafi et al., 2014b) it is tempting to speculate that adhesive signaling may be affected by loss of Tor1a-Klhl14 binding.

Chapter 3

Developmental Timing and Candidate Genes of GABApre neurons

3.1 Introduction

Our finding that the GABApre neuron population can be further restricted by developmental timing and novel GABApre candidate gene expression may be used to better identify and study GABApre circuitry.

3.2 Identity of early *Ptf1a*-derived interneurons

Inhibitory interneurons in the dorsal horn consist of several subpopulations of cells that express a wide variety of factors, such as neuropeptide Y (NPY), enkephalin (pENK), and glycine (Todd, 1996; Betley et al., 2009; Polgar et al., 2013). Functionally, these cells modulate cutaneous sensory modalities such as nociception (pain) and mechanosensation (touch) (Abraira and Ginty, 2013). Previous EM studies revealed presynaptic inhibition on cutaneous afferents in the dorsal horn (Réthelyi et al., 1982) by analyzing the presence of GABAergic and glycinergic axo-axonic contacts on sensory afferent terminals (Watson et al., 2002; Watson, 2003). This suggests that besides GABApre neurons that form boutons on proprioceptive terminals in the ventral horn, there is also a dorsal population of presynaptic inhibitory interneurons that form boutons on cutaneous terminals. While both populations are *Ptf1a*-derived and form presynaptic contacts, one population

targets proprioceptive terminals, and the other targets cutaneous terminals (Betley et al., 2009).

Using differential timing of birth to label neurons, subpopulations of premotor interneurons were successfully segregated (Tripodi et al., 2011; Benito-Gonzalez and Alvarez, 2012). Since there are at least two subpopulations of presynaptic inhibitory interneurons that are *Ptf1a*-derived, those that contact cutaneous afferents and those that contact proprioceptive afferents, can we also use timing of *Ptf1a* expression to segregate subpopulations of presynaptic interneurons? To segregate subpopulations of presynaptic inhibitory interneurons, we used timed TM injections at an early time point of e9.5 and a late time point of e12.5 in *Ptf1a*^{CreER}*; R26*^{tdTomato} mice. We found that the majority of the early-labeled population had cell bodies positioned in the dorsal spinal cord. By analyzing the expression of GABAergic synaptic markers in all early-labeled synapses in the dorsal horn, we found that the majority of dorsal horn synapses labeled in e9.5 TM injected mice expressed GAD67 (Fig. 3.1). Analyzing the expression of peptidergic markers such as NPY and pENK in these early-labeled synapses was difficult due to inefficient antibody labeling in the dorsal horn.

The majority of labeled synapses analyzed in the dorsal horn of early TM injected mice expressed GAD67, and we asked what were the targets of these labeled synapses. Since GABAergic contacts are found on cutaneous afferents (Todd, 1996; Watson, 2003; Betley et al., 2009), we analyzed whether early-labeled synapses in the dorsal horn were targeting cutaneous afferents. To analyze the targeting of dorsal inhibitory interneurons we used timed TM injections at e9.5 in *Ptf1a*^{CreER}*; R26*^{tdTomato} mice in

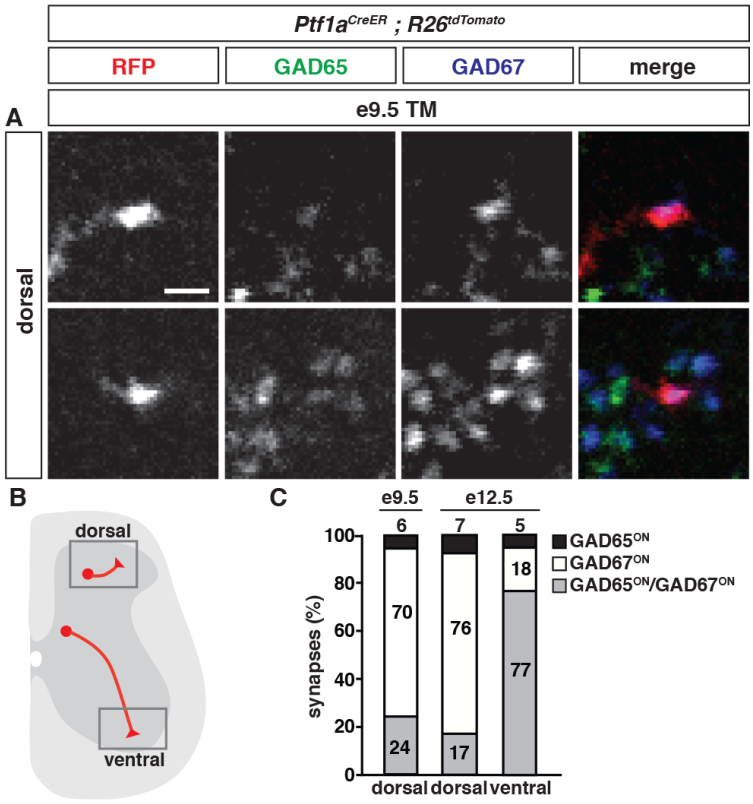

Figure 3.1: Synaptic identity of early e9.5 TM labeled synapses

(A) e9.5 TM labeled cells reside in the dorsal horn where they form GABAergic synapses labeled with GAD65 and GAD67. Scale bar: 2 µm.

(B) Diagram of neurons in the dorsal horn also forming contacts in the dorsal horn, in contrast to GABApre neurons which reside in the intermediate spinal cord but form contacts in the ventral horn.

(C) The majority of e9.5 TM labeled dorsal synapses analyzed expressed GAD67 (70%). e12.5 TM labeled dorsal synapses also expressed GAD67 (76%), while labeled ventral synapses expressed both GAD65 and GAD67 (77%).

conjunction with CTb labeling of cutaneous afferents. We found tdTomato labeled presynaptic contacts on cutaneous afferents in the dorsal horn of e9.5 TM injected mice, although we were unable to determine the neurotransmitter expression in these presynaptic contacts due to the extremely low frequency of tdTomato labeled contacts on CTb labeled afferents (Fig. 3.2). A major impediment to TM labeling at e9.5 was the embryo lethality caused by TM injections into pregnant dams at such an early time point in development. As a result the dose of TM had to be dropped which resulted in fewer tdTomato labeled cells with e9.5 TM injections compared to e12.5. Hence, the incidences of e9.5 TM labeled synapses adjacent to CTb labeled cutaneous afferents were extremely rare. However, our data nevertheless suggests that early TM injection labels cutaneous presynaptic neurons, while only late TM injection labeled GABApre neurons.

3.3 Novel GABApre interneuron genes

In locomotor circuits, interneuronal diversity is essential in controlling specific aspects of movement. Genetic screens identified subpopulations of interneurons with distinct gene expression patterns that localize in highly unique positions along the rostrocaudal and mediolateral axes of the spinal cord (Bikoff et al., 2016). While *Ptf1a* is a marker for dorsal inhibitory interneurons, there is no specific marker of GABApre neurons. To identify distinct and novel genes expressed in GABApre neurons, we conducted a microarray screen for genes specifically upregulated in the intermediate spinal cord where GABApre cell bodies are thought to reside (Jankowska et al., 1981; Hughes et al., 2005; Betley et al., 2009). We used *in silico* screening on

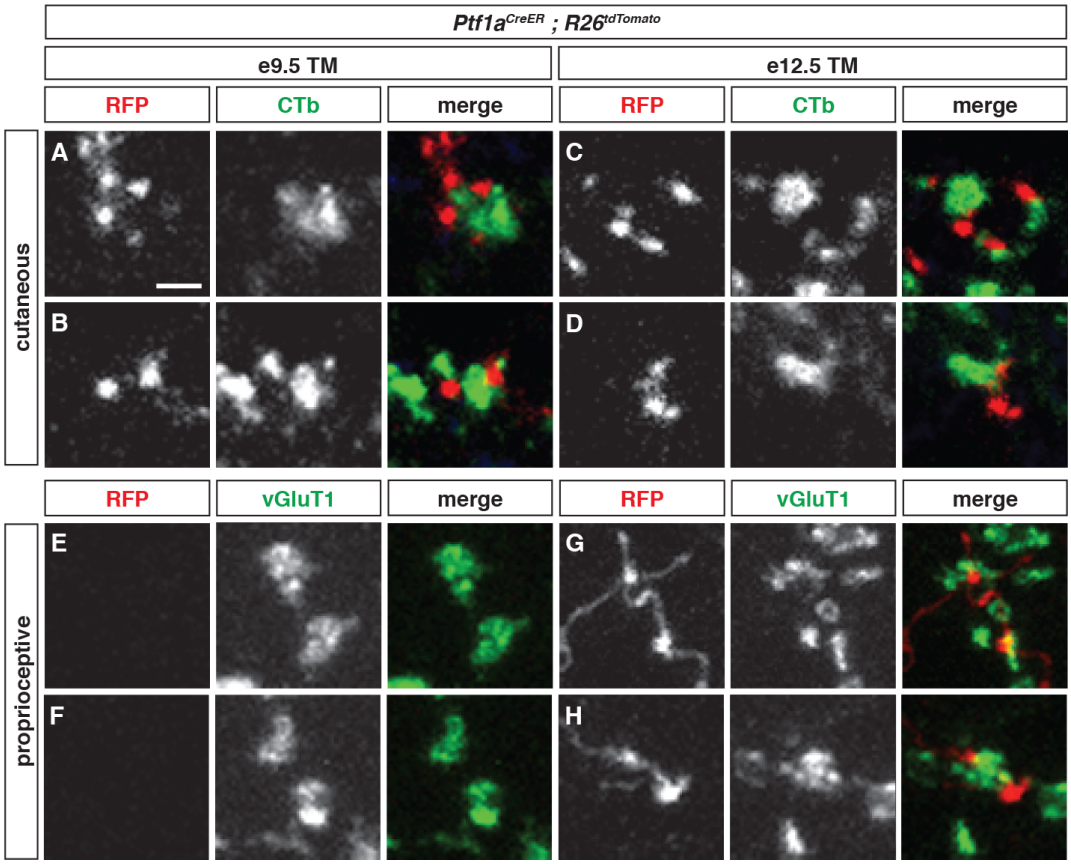

Figure 3.2: Targeting of early and late labeled *Ptf1a*-derived neurons

(A, B) Early e9.5 TM labeled neurons form contacts (red) onto CTb labeled (green) cutaneous afferents.

(C, D) Some late e12.5 TM labeled neurons (red) also form cutaneous contacts (green).

(E, F) No e9.5 TM labeled neurons project to the ventral horn and form contacts on vGluT1 labeled proprioceptive terminals (green).

(G, H) Only e12.5 TM labeled neurons (red) project to the ventral horn and form contacts on proprioceptive terminals (green). Scale bar: 2 µm.

the Allen Brain Atlas expression database to confirm any intermediate enriched candidate genes and identified *Klhl14*, which we localized to GABApre neurons, and 10 other candidates that had intermediate restricted expression in the spinal cord. The other intermediate restricted genes are ankyrin repeat and SOCS box containing 4 (*Asb4*), CART prepropeptide (*Cartpt*), coiled-coil domain containing 109b (*Ccdc109b*), cadherin 7, type 2 (*Cdh7*), crystallin mu (*Crym*), neurogenic differentiation 1 (*Neurod1*), nephronectin (*Npnt*), retinoic aid receptor, beta (*Rarb*), shisa family member 3 (*Shisa3*), and transcription factor AP-2 beta (*Tfap2β*). These genes serve a variety of cellular functions that include DNA binding, ion binding, and hormone binding. In the next section I would like to focus on two genes, *Crym* and *Tfap2β* that have been previously identified by other candidate screens in the lab and have exclusive intermediate gene expression.

Crym is a hormone binding protein with enzymatic function that was first discovered in the eye lens of marsupials where it protects against oxidative stress (Wistow and Kim, 1991). It is expressed in striatal neurons in the brain, where it binds thyroid hormone and has a neuroprotective effect from Huntington's disease (Francelle et al., 2015). Previous work in the lab has analyzed *Crym* expression in the spinal cord, and found it expressed at e18.5, p5 and turned off by p30 in the adult mouse (Fig. 3.3, Lathan McCall and Julia Kaltschmidt, unpublished). *Crym* is expressed in inhibitory interneurons, revealed by the fact that *Crym* expression is abolished in spinal cords null for *Ptf1a* (*Ptf1a*$^{Cre/Cre}$) (Fig. 3.3, Lathan McCall and Julia Kaltschmidt, unpublished). To further localize *Crym* to GABApre neurons, *Crym* expression would be evaluated in *Ptf1a*-derived neurons in the intermediate spinal cord of

Ptf1a^{Cre}*; R26*^{tdTomato} mice, since *Ptf1a* expression is fairly unique to GABApre neurons in the intermediate region (Fink et al., 2014). Also, given that we found that late TM labeled *Ptf1a*-derived cells in the intermediate spinal cord are likely GABApre neurons, we would analyze *Crym* expression in late *Ptf1a*-derived cells in the intermediate spinal cord to determine whether Crym is expressed in GABApre neurons.

To further study *Crym* expression and function, a *Crym*^{Cre} line is available (http://www.informatics.jax.org/allele/MGI:5632478) that when crossed to a conditional fluorescent reporter mouse line, would permanently label *Crym* expression in cells and synapses. This will further reveal whether *Crym* expressing cells are GABApre neurons, and form boutons on sensory afferent terminals, and whether *Crym* is expressed in all GABApre neurons or a subset. If *Crym* is expressed in GABApre neurons, *Crym* conditional knockout mouse lines may be used to analyze the consequence of loss of *Crym* expression in GABApre neurons and their circuitry. Loss of *Crym* expression in GABApre neurons may result in changes in GABApre development and circuitry due to oxidative stress.

The other identified candidate gene that was also previously studied in the lab due to its intermediate gene expression is *Tfap2β. Tfap2β* is part of the AP-2 family of transcription factors, which form dimers to bind to DNA sequences. In the retina, transcription factor *Tfap2β* has been identified to be downstream of *Ptf1a* and important for the differentiation of amacrine cells during development (Jin et al., 2015). In the spinal cord, *Tfap2β* is also downstream of *Ptf1a* and expressed during embryonic and early postnatal development. Previous work in the lab has shown *Tfap2β* to be expressed at

e18.5 and p5 (Lathan McCall and Julia Kaltschmidt , unpublished, Wildner et al., 2013). *Tfap2β* expression was also identified to be *Ptf1a* dependent, and expressed in inhibitory interneurons (Fig. 3.3). To localize *Tfap2β* expression in GABApre neurons, previous work in the lab scored co-expression of GFP positive cells with *Tfap2β* in *Gad65::^{N45}GFP*. 40% of GFP positive cells expressed *Tfap2* β at p6 (Laura McCormick, Lathan McCall and Julia Kaltschmidt, unpublished). Analysis of GFP co-expression with *Ptf1a* in *Ptf1a^{Cre}; R26^{LacZ}* mice revealed that while all GABApre terminals expressed GFP, there is extra expression of GFP in the dorsal spinal cord of *Gad65::^{N45}GFP* mice (Betley et al., 2009). While this experiment provided the first insight into whether *Tfap2β* is expressed in GABApre neurons, to further restrict *Tfap2β* expression in GABApre neurons, we analyzed *Tfap2β* expression in late *Ptf1a*-derived cells in the intermediate spinal cord.

We first analyzed *Tfap2β* expression in *Ptf1a*-derived cells in *Ptf1a^{Cre}*; *R26^{tdTomato}* mice and found that 37% of RFP labeled cells co-expressed *Tfap2β* in the intermediate spinal cord. To further assess *Tfap2β* expression as it relates to early and late *Ptf1a*-derived cells, we used early (e9.5) and late (e12.5) timed TM injections in *Ptf1a^{CreER}; R26^{tdTomato}* mice. *Tfap2β* expression was identified in tdTomato labeled cells in the intermediate spinal cord in both early and late TM injected *Ptf1a^{CreER}; R26^{tdTomato}* mice (Fig. 3.4). Taken together, these data show that *Tfap2β* is likely expressed in GABApre neurons, in addition to other subtypes of interneurons. To further study *Tfap2β* expression and function in GABApre neurons, transgenic mouse lines such as a cre line or conditional KO line would need to be created. Using a mutant mouse with conditional *Tfap2β* KO in GABApre neurons may result in neurons

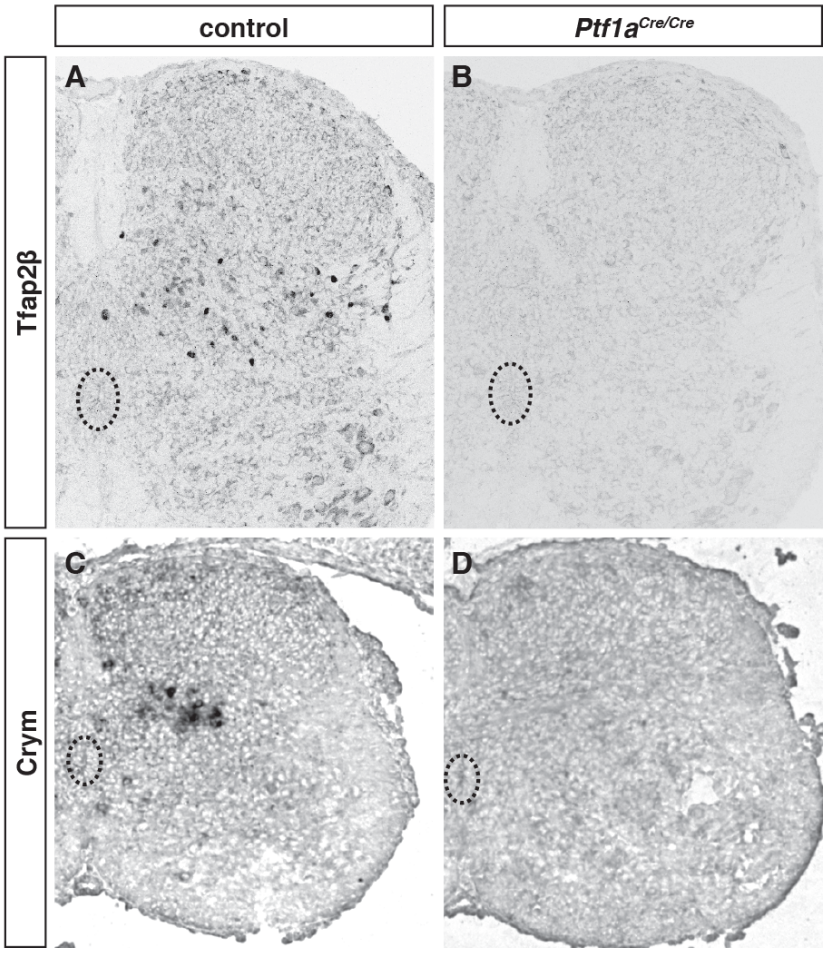

Figure 3.3: *Tfap2β* and *Crym* expression

(A) *Tfap2β* expression in e18.5 control spinal cord.

(B) No *Tfap2β* expression in e18.5 spinal cord null for *Ptf1a*.

(C) *Crym* expression in e17.5 control spinal cord. Lathan McCall and Julia Kaltschmidt, unpublished.

(D) No *Crym* expression in e17.5 spinal cord null for *Ptf1a*. Lathan McCall and Julia Kaltschmidt, unpublished.

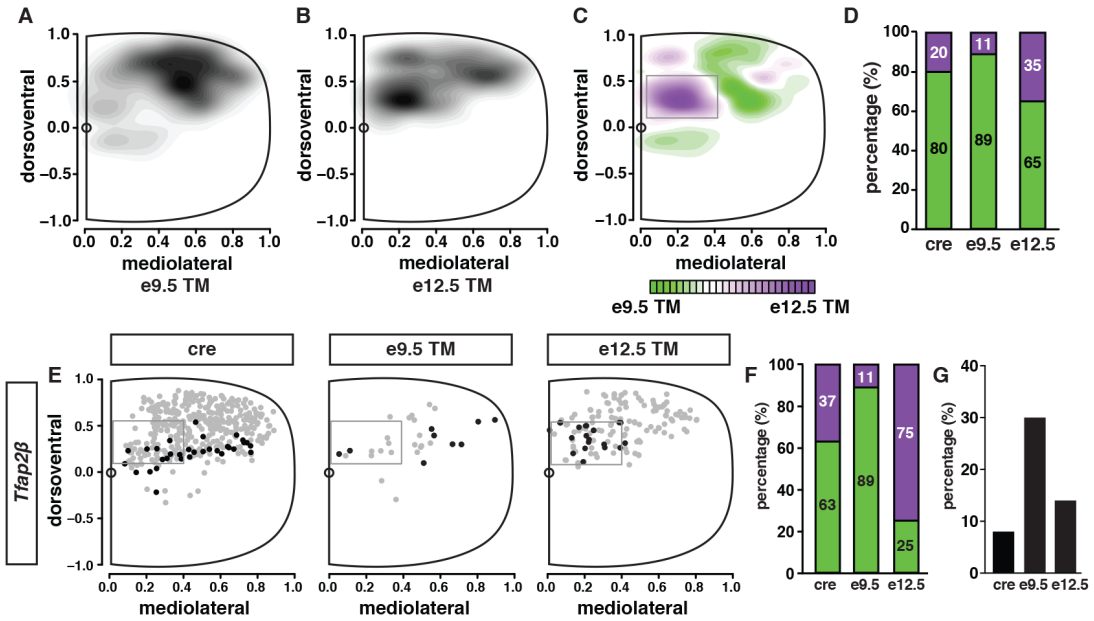

Figure 3.4: Timing of *Tfap2β* expression in *Ptf1a*-derived cells

(A, B) Density map of cell body distribution in *Ptf1a*^{CreER}; *R26*^{tdTomato} e9.5 TM injected tissue at e18.5 (A). Density map of cell body distribution in *Ptf1a*^{CreER}; *R26*^{tdTomato} e12.5 TM injected tissue at e18.5 (B).

(C) Subtraction map of e9.5 TM density map (A) and e12.5 TM density map (B), with green areas showing more e9.5 TM density and purple areas showing more 12.5 TM density. White areas show even density distribution between e9.5 TM map and e12.5 TM map. Purple box in the intermediate spinal cord is uniquely e12.5 TM density distribution, where GABApre cell bodies may be enriched.

(D) There is three-fold enrichment for intermediate cell body positioning within the box in e12.5 TM injected tissue compared to e9.5 TM injected tissue.

(E, F) *Tfap2β* is expressed in the intermediate spinal cord (E). This expression is enriched with 75% of RFP and *Tfap2β* double-labeled cells in the box in *Ptf1a*^{CreER}; *R26*^{tdTomato} e12.5 TM injected tissue (F).

(G) Overall percent of *Ptf1a*-derived cells labeled with RFP that express *Tfap2β* in early and late TM injected tissue. There are RFP/*Tfap2β* double labeled cells in e9.5 TM injected tissue (30%).

changing fates or failing to develop properly due to the fact that *Tfap2β* is a transcription factor, participating in the developmental programming of cells.

Taken together, the GABApre population can be further restricted by late *Ptf1a* expression, while some early *Ptf1a* expressing cells seem to be GABAergic and contact cutaneous afferents. Furthermore, GABApre candidate genes, *Crym* and *Tfap2β* are promising due to their dependence on *Ptf1a* expression, and their exclusive expression in the intermediate spinal cord. Further studies may be conducted to localize their expression in GABApre neurons.

Chapter 4

Concluding Remarks and Future Directions

4.1 Introduction

My thesis work investigated the expression of *Klhl14* in GABApre neurons, and the link between GABApre neurons and motor disease in the spinal cord. GABApre neurons exert presynaptic inhibition on proprioceptive sensory afferents in the sensory-motor circuit, and deficits in presynaptic inhibition have been demonstrated in many different motor diseases such as dystonia and Parkinson's disease. However, the contribution of GABApre neurons to motor disease is largely unstudied. This has been especially difficult to study due to the lack of specific markers of GABApre neurons that could be used to target them. We set out to identify novel GABApre genes with a focus on those that may be involved in a motor disease. We performed a microarray screen at p6 when GABApre boutons are first formed (Betley et al., 2009), and compared upregulated genes in the intermediate spinal cord to those expressed in the dorsal and ventral horn. We thereby identified *Klhl14* to be highly expressed in the intermediate region. To further evaluate to what extent *Klhl14* expression is restricted to GABApre neurons, we used our finding that GABApre neurons are a late *Ptf1a*-derived population, and identified *Klhl14* expression to localize to late *Ptf1a*-derived GABApre neurons. Klhl14 binds Tor1a, which is implicated in dystonia. In a mouse mutant for *Tor1a*, *Dyt1 Δ E,* in which Klhl14 and Tor1a binding is disrupted but not entirely abolished, we identified a 20% reduction in the number of GABApre boutons on sensory afferent terminals when compared to controls. The molecular

mechanisms that lead to GABApre bouton loss in *Dyt1 ΔE* mutant mice, as well as the functional consequences of this loss remain unresolved. In this chapter we will address future directions and experiments to further our developmental and genetic understanding of GABApre interneurons and how their circuitry is disrupted due to the *Dyt1 ΔE* mutation.

4.2 Timing of neurogenesis of *Ptf1a*-derived interneurons

Dorsal interneurons are born from six dorsal progenitor domains in the developing mouse embryo (Caspary and Anderson, 2003; Helms and Johnson, 2003). There are two waves of neurogenesis with early neurogenesis occurring at e10-e11.5, and late neurogenesis occurring at e12-e14.5. Dorsal inhibitory interneurons are born in the dI4 domain during early neurogenesis, and in the dILA domain during late neurogenesis (Gross et al., 2002; Müller et al., 2002).

Dorsal inhibitory interneurons from both the dI4 domain as well as the dILA domain express the transcription factor *Ptf1a* (Glasgow et al., 2005; Wildner et al., 2013). *Ptf1a* expression is post-mitotic and temporally restricted during mouse development, turning on at e10.5 and turning off after e13.5 (Fig. 4.1, Glasgow et al., 2005; Mizuguchi et al., 2006). *Ptf1a* expression turns on after neurogenesis, but the exact correlation between timing of neurogenesis of a neuron and timing of *Ptf1a* expression is unknown. For example, it is not known when a neuron, born at e10, expresses *Ptf1a* after its birth, and whether that timing is exactly the same for each neuron. To verify that late *Ptf1a*-derived neurons are also later born cells, we would use

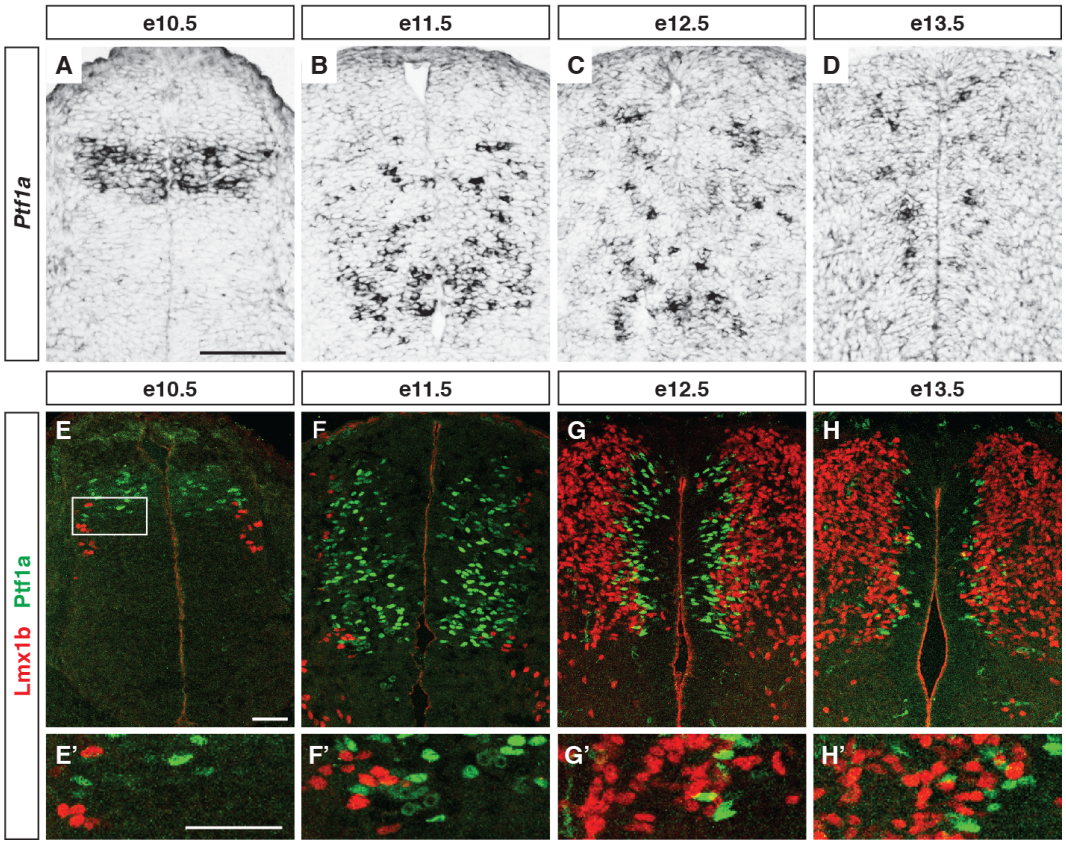

Figure 4.1: Timeline of *Ptf1a* expression

(A-D) *In situ* hybridization of *Ptf1a* expression in mouse developing spinal cord from e10.5 to e13.5. No expression is seen before or after these time points. Scale bar: 100 µm.

(E-H) Antibody labeling of Ptf1a expression with Lmx1b (marker for dI5 and dILB). There is no colabeling between Ptf1a and Lmx1b. Ptf1a is expressed in dI4 at e10.5 and e11.5, above dI5. Ptf1a expression expands in dILA, which intermingles with dILB in a salt and pepper fashion at e12.5 and e13.5. Scale bars: 50 µm.

bromodeoxyuridine (BrdU) to assign timing of birth to *Ptf1a*-derived cells. Since BrdU labels dividing cells, we would inject BrdU at e9.5 or e12.5 into pregnant $R26^{tdTomato}$ dams that were crossed with $Ptf1a^{Cre}$ animals so that the pups would have all *Ptf1a*-derived cells fluorescently labeled. BrdU and RFP double-labeled cells would enable us to map cell body positioning to timing of birth of *Ptf1a*-derived neurons. If both early and late BrdU injections labeled cells in a similar cell distribution to our TM labeling at the same time points, it would correlate timing of birth with timing of *Ptf1a* expression (Fig. 4.2). This would confirm that late born *Ptf1a*-derived cells in dILA, some of which are GABApre neurons, also express *Ptf1a* late. If we do not see similar cell distributions between timed BrdU labeling and timed TM labeling, it would suggest that the timing of birth and the subsequent timing of *Ptf1a* expression are not correlated, and that different cells could be expressing *Ptf1a* at varying time points after they are born.

4.3 Disrupted Klhl14 and Tor1a binding due to *Dyt1ΔE* mutation

Identifying genetic markers of GABApre neurons may further our understanding of their role in motor disease. Our analysis of a mutant mouse for dystonia, *Dyt1 Δ E*, revealed a loss of GABApre bouton number on sensory afferent terminals. The *Dyt1 Δ E* mutation results in disrupted binding between the mutant Tor1a protein and its cofactor Klhl14 (Giles et al., 2009). *Klhl14* is highly conserved amongst humans and rats with 99% similarity of amino acid identity (Giles et al., 2009). Tor1a protein is broadly distributed, although there are only neural-based deficits observed with *Tor1a* mutations in humans

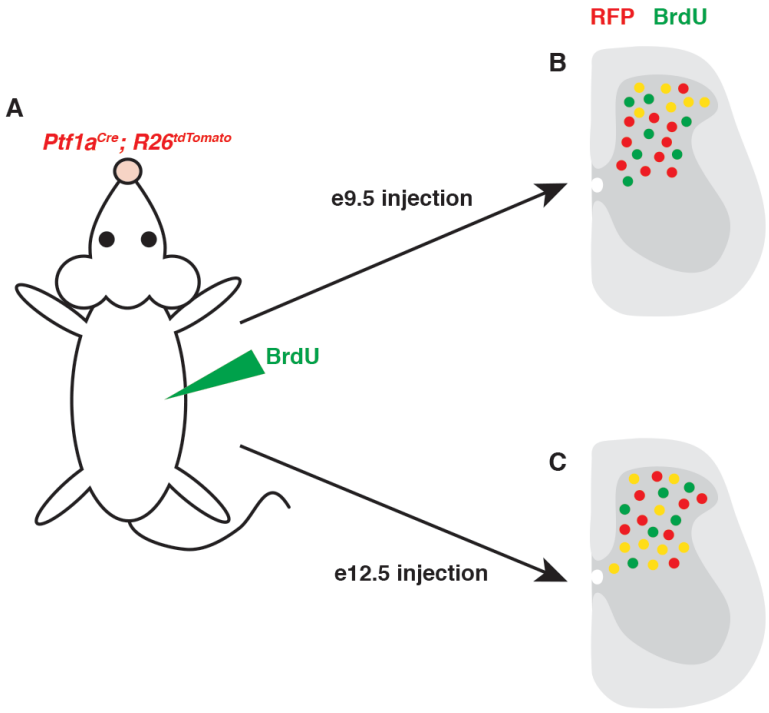

Figure 4.2: Using BrdU to assign timing of birth to *Ptf1a*-derived neurons

(A) BrdU is injected into pregnant *Ptf1a*^{Cre}*; R26*^{tdTomato} dams at e9.5 and e12.5 when our TM injections were also done.

(B) We expect e9.5 BrdU injections to label RFP-positive cells in the dorsal spinal cord, suggesting that early born Ptf1a-derived cells settle in the dorsal horn, confirming our e9.5 TM labeling.

(C) We expect e12.5 BrdU injections to label RFP-positive cells in the intermediate spinal cord as well as in the dorsal horn. This suggests that only late born *Ptf1a*-derived neurons have intermediate cell body positioning and are likely GABApre neurons, confirming our e12.5 TM labeling.

(Breakefield et al., 2008). Within a cell, Tor1a is localized to the nuclear envelope (NE) (Goodchild et al., 2005), endoplasmic reticulum (ER) (Callan et al., 2007), and it has been found in synaptic terminals (Granata et al., 2008). Klhl14 and Tor1a codistribute in neural tissues. For example, colocalization of Klhl14 and Tor1a were found in the ER of human-derived cells in cell culture (Giles et al., 2009). While the *Dyt1 ΔE* mutation significantly reduces binding between Klhl14 and Tor1a, this mutation does not completely abolish it (Giles et al., 2009).

Synaptic abnormalities have been observed both *in vitro* and *in vivo* due to the *Dyt1 ΔE* mutation. *In vivo* studies using *Dyt1 ΔE* mutant mice revealed decreased probability of synaptic vesicle release in hippocampal slices, supporting the work in cell culture showing deficits in synaptic vesicle recycling. Furthermore, there was a significant reduction in the frequency of sEPSCs, signaling a presynaptic release deficit. There was no change in miniature (m)EPSCs, which are action-potential independent (Yokoi et al., 2013). This suggests that an action-potential dependent presynaptic release deficit is present in *Dyt1 ΔE* mutants.

In vitro studies using cell culture showed that Tor1a binds snapin (Granata et al., 2008), an important protein for vesicle exocytosis by improving the interaction of the SNARE complex with Syt1 (Ilardi et al., 1999). The *Dyt1 ΔE* mutation causes the accumulation of Syt1 on the plasma membrane at synapses and hindered synaptic vesicle recycling overall (Granata et al., 2008, 2011).

Since the *Dyt1 ΔE* mutation has been shown to cause the accumulation of Syt1 at the cell membrane of synapses, changes in Syt1 levels in GABApre

boutons may be indicative of deficits in synaptic machinery that may lead to synapse loss or dysfunction. Tor1a may play a role stabilizing synaptic machinery, and mutant Tor1a may destabilize synapses causing them to not form or to retract (Granata et al., 2008, 2011). To evaluate changes in Syt1 levels in GABApre boutons in *Dyt1 Δ E* mice, we will intercross *Ptf1a*^{Cre} with *R26*^{tdTomato} mice on the *Dyt1 Δ E* background to fluorescently label GABApre boutons, and colabel them with RFP and Syt1 to measure Syt1 intensity levels on vGluT1 terminals in wt and *Dyt1 Δ E* mutant mice. As a control, due to the fact that GAD67 is cytoplasmic and not associated with synaptic machinery, we will also analyze the protein levels of GAD67 at the synapse. We expect to see no change in GAD67 levels in GABApre boutons in *Dyt1 Δ E* mice (in collaboration with Jarret Weinrich).

4.4 Analysis of a Klhl14 mutant

The previous studies on synaptic abnormalities observed in the *Dyt1 Δ E* mutation have been solely focused on *Tor1a.* Recent work has revealed that Tor1a interacts with *Klhl14*, and that the *Dyt1 Δ E* mutation disrupts Tor1a-Klhl14 binding (Giles et al., 2009). While very little is known about the function of Klhl14, other members of the kelch-like family proteins have been found to bind actin and play a role in synaptogenesis (Perissinotti et al., 2015). Therefore to gain a better understanding of the function of Klhl14 protein and its expression in neurons, a classic approach would be to label *Klhl14*-expressing cells and their processes and study the consequences of a loss-of-function of *Klhl14* in GABApre interneurons.

To label *Klhl14*-expressing cells and their processes, mouse genetics may to be used. To permanently label *Klhl14*-expressing cells, a mouse line in which *Klhl14* drives cre expression, *Klhl14*^{Cre} would permanently label all *Klhl14*-expressing cells and their synapses when crossed to a fluorescent reporter line such as *R26*^{tdtomato}. The presence of fluorescently labeled boutons on sensory terminals in the ventral horn along with their co-expression of GABApre markers, such as GAD65, GAD67, and Syt1 would verify that fluorescently labeled *Klhl14*-expressing cells are GABApre neurons (Fig. 4.3A). Additionally this experiment will tell us whether *Klhl14* is expressed in all GABApre neurons, or just a subset, and whether its expression is exclusively in GABApre neurons or also in other inhibitory spinal interneurons.

To evaluate the role of *Klhl14* in neural circuitry and GABApre neurons with a conditional KO mouse line of *Klhl14*, we would generate a floxed *Klhl14* mutant and intercross it with the *Ptf1a*^{Cre} mouse line, which expresses cre in all *Ptf1a*-derived cells. Based on the restricted expression of *Klhl14*, we predict that this conditional *Klhl14* KO mouse may highly target GABApre cells (Fig. 4.3B). By analyzing GABApre bouton circuitry in these mutant mice, we would evaluate whether the synaptic deficits observed in *Dyt1 ΔE* mutants are solely due to mutated *Tor1a* or due to interrupted Tor1a-Klhl14 binding. Since there are no sensory-motor deficits observed in *Dyt1 ΔE* mice, the changes in GABApre circuitry are likely due exclusively to GABApre dysfunction. If we see a similar 20% or greater loss of GABApre boutons at p21 in *Klhl14* mutant mice, it would reveal that Tor1a-Klhl14 binding is necessary for GABApre bouton formation. If no change in GABApre bouton number is seen in these *Klhl14* mutants, it is likely that GABApre bouton loss is exclusively due to

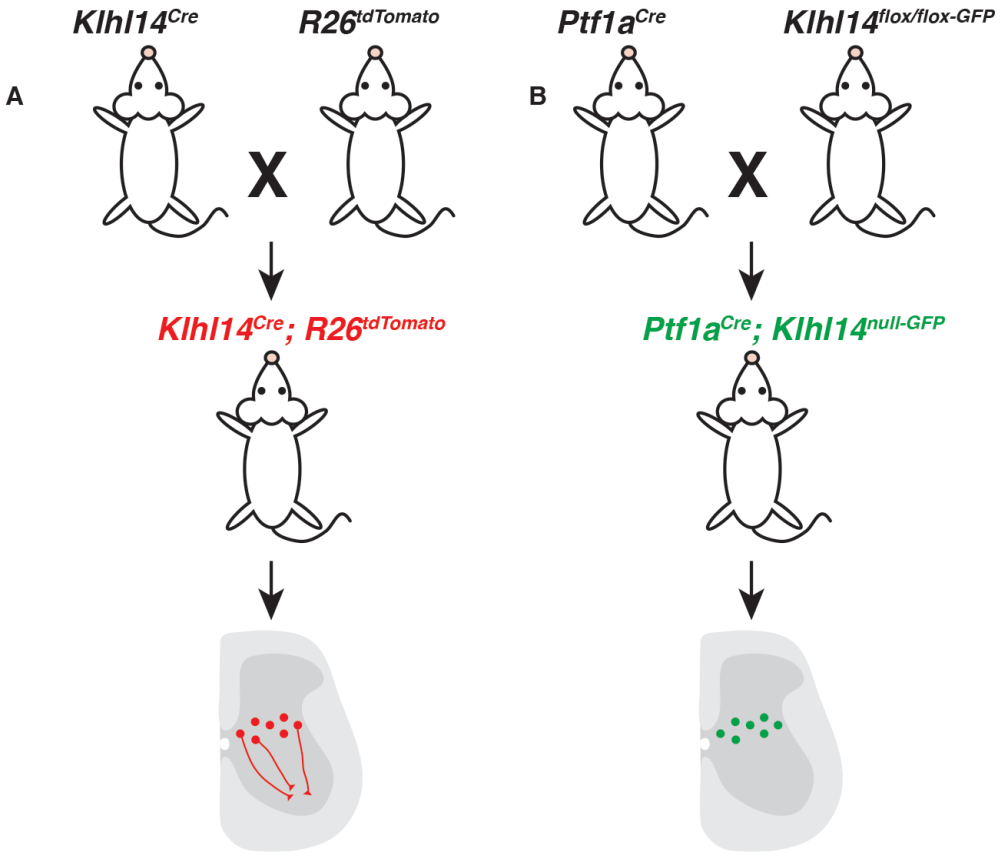

Figure 4.3: Mouse lines to better study *Klhl14* expression and function

(A) *Klhl14*^{Cre} mice intercrossed with *R26*^{tdTomato} mice have *Klhl14* expressing neurons and projections labeled. Some if not all of these cells may be GABApre neurons.

(B) Conditional *Klhl14* KO reporter mice intercrossed with *Ptf1a*^{Cre} mice are null for *Klhl14* in *Ptf1a*-derived cells, which are labeled with a fluorescent protein reporter such as GFP.

Tor1a dysfunction in *Dyt1ΔE* mice. If *Klhl14* mutants do exhibit changes in GABApre circuitry, behavioral testing such as studying gain control would be conducted, which is elaborated further in a later section of this thesis.

4.5 Descending pathways in dystonia

Most of the research conducted on understanding dystonia is focused on neural circuit dysfunction in the brain, which investigators believe to be the source of dystonic symptoms. *Tor1a* is highly expressed throughout the CNS, including the cerebral cortex, basal ganglia, and cerebellum (Shashidharan et al., 2000; Granata et al., 2009; Puglisi et al., 2013). Especially high expression of *Tor1a* is observed in dopaminergic neurons in the substantia nigra in humans, suggesting a link between dopamine signaling and *Dyt1* mutations (Farrell et al., 2009; Sciamanna et al., 2012; Pappas et al., 2015). Furthermore, some forms of dystonia are dopa responsive and treatment with L-dopa help ameliorate symptoms of the disorder (Breakefield et al., 2008), revealing that abnormal levels of dopamine in the striatum can result in the symptoms of dystonia.

There have been many fewer studies examining spinal circuitry dysfunction in dystonia, and these studies in the spinal cord were restricted to H-reflex testing in human patients of dystonia. Nakashima et al. (1989) found increased H-reflexes due to decreased presynaptic inhibition in human patients with dystonia compared to controls, and postulated that this could be due to basal ganglia dysfunction, which results in disrupted descending control of spinal interneurons (Nakashima et al., 1989). The basal ganglia does not

form direct contacts in the spinal cord (Nelson and Kreitzer, 2014), but the basal ganglia does project to the cortex and the corticospinal tract (CST). Dysfunctional basal ganglia input could be affecting CST neurons, which have been shown to directly contact putative GABApre neurons (Russ et al., 2013). Since *Tor1a* is expressed in the cortex (Shashidharan et al., 2000), and CST neurons reside in the cortex and project to the spinal cord (Welniarz et al., 2015), *Tor1a* could be expressed in CST neurons that provide input to GABApre neurons.

To localize *Tor1a* in CST neurons, novel viral tracing techniques may be used to retrogradely label CST neurons from their contacts on GABApre neurons in the spinal cord. Basaldella et al. (2015) used viral tracing technology to identify projection neurons from the spinal cord to the brain. By conducting intraspinal injections of G-protein deficient rabies viruses encoding fluorescent protein markers (Basaldella et al., 2015) into the intermediate spinal cord where GABApre cell bodies reside, we would retrogradely label CST neurons in $Ptf1a^{Cre}$; $R26^{tdTomato}$ mice. By labeling the precise cortical neurons that contact GABApre cell bodies, we would identify whether these cortical neurons express *Tor1a*. Furthermore carrying out this technique would also serve as a means to evaluate potential changes in connectivity between labeled CST neurons and labeled GABApre neurons in $Ptf1a^{Cre}$; $R26^{tdTomato}$ mice on wt and *Dyt1 ΔE* background.

In *Dyt1 ΔE* mice, mutant *Tor1a* in CST neurons could be affecting their input on GABApre neurons. To visualize CST input, $Emx1^{GFP}$ mice would be used, in which *Emx1* drives GFP expression in all cortical neurons (Hantman and Jessell, 2011). To determine whether GABApre neurons have disrupted

CST input in *Dyt1 ΔE* mice, *Emx1*^{GFP} mice would be crossed with *Ptf1a*^{Cre}; *R26*^{tdTomato} mice on the *Dyt1 ΔE* background to analyze CST projections and contacts on putative GABApre cell bodies in the intermediate spinal cord (Hantman and Jessell, 2011). Previous work has shown that disrupted CST input on putative GABApre cell bodies in a mouse model for perinatal stroke showed no loss in GABApre bouton number (Russ et al., 2013), so our loss of GABApre bouton phenotype may be due exclusively to GABApre dysfunction.

Recently, the translational relevance of certain *Dyt1 ΔE* mouse models of dystonia has come into question. *Dyt1 ΔE* mutant mice seem to lack dystonic symptoms such as persistent co-contraction of muscles and involuntary twisting movements. Instead, these mice exhibit other abnormal movements such as deficits in beam walking and hyperactivity (Dang et al., 2006). Due to the fact that *Dyt1 ΔE* is a loss-of-function mutation, recent work has studied a conditional *Tor1a* KO in the brain as a mouse model for dystonia. Deletion of *Tor1a* in cholinergic and GABAergic progenitors in the forebrain and striatum caused motor abnormalities in mice during juvenile CNS maturation, which better represented the symptoms exhibited in human patients of dystonia (Pappas et al., 2015). In these mutant mice, abnormal motor behaviors of twisting and limb clasping were observed, and worsened as the mice matured. Antimuscarinic drugs were effective at mitigating these motor defects, suggesting abnormal cholinergic signaling in these mutant mice. Furthermore, GABAergic cell number was not affected in the striatum, but cholinergic cell number was deficient, due to cholinergic cell death (Pappas et al., 2015). While the cholinergic system was well studied in this mutant mouse, the contributions of *Tor1a* loss in GABAergic cells was not

elucidated beyond a cell number analysis that showed no cell death. Furthermore, any changes in overall neural circuitry of inhibitory neurons was not addressed, even though other studies have suggested that GABAergic synaptogenesis is impaired in cerebellum in other mouse models for dystonia (Vanni et al., 2015).

If the conditional *Tor1a* KO mutant described in Pappas et al. (2015) is a more accurate mouse model of dystonia, we would evaluate deficits in presynaptic inhibition in this line. To evaluate potential changes in GABApre circuitry, *Tor1a* conditional KO mice would be crossed to *Ptf1a*^{Cre} mice in order to selectively KO *Tor1a* in *Ptf1a*-derived cells and GABApre neurons. We would then check for proper GABApre bouton formation.

4.6 Behavioral testing and function

While studying the changes in neural circuitry deficits in mouse models of dystonia may provide insight into the causes of the disorder, behavioral testing would verify the translational relevance of mouse models of dystonia. Although there has been some work reconciling the motor symptoms observed in human patients with relevant mouse models (Pappas et al., 2015), further behavioral testing of presynaptic inhibition and measuring H-reflex offer additional insights. In human patients of dystonia, H-reflex testing has shown decreased presynaptic inhibition (Nakashima et al., 1989; Panizza et al., 1990). To test whether deficits in presynaptic inhibition may be observed in mouse models of dystonia several mouse lines such as the conditional *Tor1a* KO mouse as well as the *Dyt1 ΔE* mice should be tested for changes in H-

reflex. A greater H-reflex observed in mice with conditional *Tor1a* KO in forebrain as described in Pappas et al., 2015 that exhibits dystonic symptoms, may further suggest that deficits in presynaptic inhibition are associated with dystonia. This study may also reveal potential deficits in presynaptic inhibition that could be due to GABApre neuron dysfunction in either forelimb or hindlimb in these mutant mice, since both limbs can be affected in human patients of dystonia (Breakefield et al., 2008). In *Dyt1 ΔE* mice, H-reflex testing may also reveal deficits in presynaptic inhibition due to loss of GABApre boutons, which would result in increased H-reflex in *Dyt1 ΔE* mice compared to wt.

Presynaptic inhibition serves as a method of providing gain control on sensory feedback (Fink et al., 2014), and deficits in presynaptic inhibition may result in abnormal gain control. Measuring the H-reflex in human studies of dystonia has been conducted in the forearm (Nakashima et al., 1989; Priori et al., 1995), while deficits in gain control in mice while executing skilled movement have been observed in the forelimb (Fink et al., 2014). To test for fine motor deficits due to gain control, mouse models of dystonia such as the conditional *Tor1a* KO and *Dyt1 ΔE* mice would be subjected to a targeted reaching assay as described in Fink et al. (2014). Deficits in gain control in these mouse models may provide a further link between GABApre neuron dysfunction that may also be due to CST defects, and the symptoms of dystonia.

Finally, electrophysiological studies may contribute to a better understanding of GABApre circuit dysfunction in mouse models of dystonia. To analyze deficits in presynaptic inhibition in mouse models for dystonia, we would record from dorsal roots to measure changes in presynaptic inhibition

and PAD. If GABApre neurons in *Tor1a* conditional KO mice or *Dyt1 ΔE* mice are dysfunctional we may see more PAD, which along with potential changes in H-reflex, may provide further evidence that GABApre neurons and changes in presynaptic inhibition may mediate symptoms associated with dystonia.

4.7 Concluding remarks

My thesis work identified enriched genes in the intermediate spinal cord, and evaluated a potential link between GABApre neurons and dystonia. Using the timeline of transcription factor *Ptf1a* expression, I showed that GABApre neurons are late *Ptf1a*-derived cells, and that GABApre neurons express *Klhl14* and its cofactor, *Tor1a*. Klhl14 and Tor1a directly bind, and this binding is disrupted in the *Dyt1 ΔE* mutated form of *Tor1a*, which has been implicated in dystonia. I demonstrated that mice carrying this *Dyt1 ΔE* mutation displayed a decrease in GABApre bouton number compared to wt mice. Although no studies have evaluated GABApre dysfunction in mediating the symptoms of dystonia, in human patients of dystonia, measuring changes in the H-reflex revealed deficits in presynaptic inhibition. Given our finding of a loss of GABApre bouton number, these deficits in presynaptic inhibition could be due to disrupted GABApre circuitry in the *Dyt1 ΔE* mutation. Taken together, these data suggest a link between GABApre neurons and dystonia.

Dystonia is widely believed to be due to circuit disorder because of the absence of any neurodegeneration, and in this chapter I have discussed current efforts as well as future directions that would provide insight into how GABApre neurons may be affected in dystonia. The generation of *Klhl14*

mutant mice may help to confirm *Klhl14* expression in GABApre neurons, and to further understand the role of *Klhl14* in GABApre bouton formation and differentiation. Moreover, testing of H-reflex in mouse models of dystonia would provide greater insight into the role and weight of presynaptic inhibition in dystonia and even other motor diseases.

Ultimately, interneurons are an incredibly heterogeneous population of cells, and interneuron dysfunction has been linked to numerous nervous system disorders. Understanding the development, circuitry, and function of specific subpopulations of interneurons will provide a greater understanding of how they participate in human disease. The final goal is the potential to develop better therapeutics to cure neural pathologies. By identifying and understanding the underlying cause of these disorders, we will be able to develop therapeutics to alleviate or even cure them.

References

Abraira VE, Ginty DD (2013) The sensory neurons of touch. Neuron 79:618–639 Available at: http://dx.doi.org/10.1016/j.neuron.2013.07.051.

Achache V, Roche N, Lamy JC, Boakye M, Lackmy A, Gastal A, Quentin V, Katz R (2010) Transmission within several spinal pathways in adults with cerebral palsy. Brain 133:1470–1483.

Alaynick WA, Jessell TM, Pfaff SL (2011) SnapShot: Spinal cord development. Cell 146:178.e1 Available at: http://dx.doi.org/10.1016/j.cell.2011.06.038.

Alvarez FJ, Fyffe REW (2007) The continuing case for the Renshaw cell. J Physiol 584:31–45.

Alvarez FJ, Jonas PC, Sapir T, Hartley R, Berrocal MC, Geiman EJ, Todd AJ, Goulding M (2005) Postnatal phenotype and localization of spinal cord V1 derived interneurons. J Comp Neurol 493:177–192.

Amin ND, Bai G, Klug JR, Bonanomi D, Pankratz MT, Gifford WD, Hinckley CA, Sternfeld MJ, Driscoll SP, Dominguez B, Lee K-F, Jin X, Pfaff SL (2015) Loss of motoneuron-specific microRNA-218 causes systemic neuromuscular failure. Sci 350:1525–1529 Available at: http://www.sciencemag.org/cgi/doi/10.1126/science.aad2509.

Arber S (2012) Motor Circuits in Action: Specification, Connectivity, and Function. Neuron 74:975–989 Available at: http://dx.doi.org/10.1016/j.neuron.2012.05.011.

Arber S, Han B, Mendelsohn M, Smith M, Jessell TM, Sockanathan S (1999) Requirement for the homeobox gene Hb9 in the consolidation of motor neuron identity. Neuron 23:659–674.

Arber S, Ladle DR, Lin JH, Frank E, Jessell TM (2000) ETS gene Er81 controls the formation of functional connections between group Ia sensory afferents and motor neurons. Cell 101:485–498.

Ashrafi S, Betley JN, Comer J, Brenner-Morton S, Bar V, Shimoda Y, Watanabe K, Peles E, Jessell T, Kaltschmidt J (2014a) Neuronal Ig/Caspr Recognition Promotes the Formation of Axoaxonic Synapses in Mouse Spinal Cord. Neuron 81:120–129.

Ashrafi S, Betley JN, Comer J, Brenner-Morton S, Bar V, Shimoda Y, Watanabe K, Peles E, Jessell T, Kaltschmidt J (2014b) Neuronal Ig/Caspr Recognition Promotes the Formation of Axoaxonic Synapses in Mouse Spinal Cord. Neuron 81:120–129 Available at: http://dx.doi.org/10.1016/j.neuron.2013.10.060.

Basaldella E, Takeoka A, Sigrist M, Arber S (2015) Multisensory Signaling Shapes Vestibulo-Motor Circuit Specificity. Cell 163:301–312 Available at: http://dx.doi.org/10.1016/j.cell.2015.09.023.

Benito-Gonzalez A, Alvarez FJ (2012) Renshaw Cells and Ia Inhibitory Interneurons Are Generated at Different Times from p1 Progenitors and

Differentiate Shortly after Exiting the Cell Cycle. J Neurosci 32:1156–1170.

Betley JN, Cao ZFH, Ritola KD, Sternson SM (2013) Parallel, redundant circuit organization for homeostatic control of feeding behavior. Cell 155:1337–1350 Available at: http://dx.doi.org/10.1016/j.cell.2013.11.002.

Betley JN, Wright CVE, Kawaguchi Y, Erdélyi F, Szabó G, Jessell TM, Kaltschmidt JA (2009) Stringent Specificity in the Construction of a GABAergic Presynaptic Inhibitory Circuit. Cell 139:161–174.

Bikoff JB, Gabitto MI, Rivard AF, Drobac E, Machado TA, Miri A, Brenner-Morton S, Famojure E, Diaz C, Alvarez FJ, Mentis GZ, Jessell TM (2016) Spinal inhibitory interneuron diversity delineates variant motor microcircuits. Cell In press:207–219 Available at: http://dx.doi.org/10.1016/j.cell.2016.01.027.

Breakefield XO, Blood AJ, Li Y, Hallett M, Hanson PI, Standaert DG (2008) The pathophysiological basis of dystonias. Nat Rev Neurosci 9:222–234 Available at: http://www.ncbi.nlm.nih.gov/entrez/query.fcgi?db=pubmed&cmd=Retrieve&dopt=AbstractPlus&list_uids=18285800.

Briscoe J, Pierani a, Jessell TM, Ericson J (2000) A homeodomain protein code specifies progenitor cell identity and neuronal fate in the ventral neural tube. Cell 101:435–445.

Brown A (1981) Organization of the spinal cord. New York.

Brown AG, Fyffe RE (1981) Direct observations on the contacts made between Ia afferent fibres and alpha-motoneurones in the cat's lumbosacral spinal cord. J Physiol 313:121–140.

Buffelli M, Burgess RW, Feng G, Lobe CG, Lichtman JW, Sanes JR (2003) Genetic evidence that relative synaptic efficacy biases the outcome of synaptic competition. Nature 424:430–434.

Burke R, Nelson P (1966) Synaptic activity in motoneurons during natural stimulation of muscle spindles. Science (80-) 151:1088–1091.

Callan AC, Bunning S, Jones OT, High S, Swanton E (2007) Biosynthesis of the dystonia-associated AAA+ ATPase torsinA at the endoplasmic reticulum. Biochem J 401:607–612 Available at: http://www.pubmedcentral.nih.gov/articlerender.fcgi?artid=1820811&tool=pmcentrez&rendertype=abstract.

Caspary T, Anderson K V (2003) Patterning cell types in the dorsal spinal cord: what the mouse mutants say. Nat Rev Neurosci 4:289–297.

Chang Q, Gonzalez M, Pinter MJ, Balice-Gordon RJ (1999) Gap junctional coupling and patterns of connexin expression among neonatal rat lumbar spinal motor neurons. J Neurosci 19:10813–10828.

Charlesworth G, Bhatia KP, Wood NW (2013) The genetics of dystonia: New

twists in an old tale. Brain 136:2017–2037.

Cheng L, Arata A, Mizuguchi R, Qian Y, Karunaratne A, Gray P a, Arata S, Shirasawa S, Bouchard M, Luo P, Chen C-L, Busslinger M, Goulding M, Onimaru H, Ma Q (2004) Tlx3 and Tlx1 are post-mitotic selector genes determining glutamatergic over GABAergic cell fates. Nat Neurosci 7:510–517.

Comi AM, Johnston M V, Wilson MA (2005) Strain variability, injury distribution, and seizure onset in a mouse model of stroke in the immature brain. Dev Neurosci 27:127–133.

Conradi S (1969) Ultrastructure and distribution of neuronal and glial elements on the motoneuron surface in the lumbosacral spinal cord of the adult cat. Acta Physiol Scand Suppl 332:5–48 Available at: http://www.ncbi.nlm.nih.gov/pubmed/4195458 [Accessed May 6, 2015].

Dang MT, Yokoi F, McNaught KSP, Jengelley TA, Jackson T, Li J, Li Y (2005) Generation and characterization of Dyt1 DeltaGAG knock-in mouse as a model for early-onset dystonia. Exp Neurol 196:452–463.

Dang MT, Yokoi F, Pence MA, Li Y (2006) Motor deficits and hyperactivity in Dyt1 knockdown mice. Neurosci Res 56:470–474.

Eccles JC, Eccles RM, Lundberg A (1957) The convergence of monosynaptic excitatory afferents on to many different species of alpha motoneurones. J Physiol 137:22–50.

Eccles JC, Eccles RM, Magni F (1961) Central inhibitory action attributable to presynaptic depolarization produced by muscle afferent volleys. J Physiol 159:147–166.

Eccles JC, Schmidt R, Willis WD (1963) Pharmacological Studies on Presynaptic Inhibition. J Physiol 168:500–530.

Eccles JC, Schmidt RF, Willis WD (1962) Presynaptic inhibition of the spinal monosynaptic reflex pathway. J Physiol 161:282–297.

Ericson J, Morton S, Kawakami A, Roelink H, Jessell TM (1996) Two critical periods of Sonic Hedgehog signaling required for the specification of motor neuron identity. Cell 87:661–673.

Farrell CA, Martin KL, Hutton M, Delatycki MB, Cookson MR, Lockhart PJ (2009) Mutant torsinA interacts with tyrosine hydroxylase in cultured cells. Neuroscience 164:1127–1137.

Fink AJP, Croce KR, Huang ZJ, Abbott LF, Jessell TM, Azim E (2014) Presynaptic inhibition of spinal sensory feedback ensures smooth movement. Nature 509:43–48 Available at: http://www.nature.com/doifinder/10.1038/nature13276.

Frank K, Fuortes MGF (1957) Presynaptic and postsynaptic inhibition of monosynaptic reflexes. Fed Proc 16:39–40.

Fukuhara K, Imai F, Ladle DR, Katayama K ichi, Leslie JR, Arber S, Jessell TM, Yoshida Y (2013) Specificity of Monosynaptic Sensory-Motor Connections Imposed by Repellent Sema3E-PlexinD1 Signaling. Cell Rep 5:748–758 Available at: http://dx.doi.org/10.1016/j.celrep.2013.10.005.

Giles LM, Li L, Chin LS (2009) Printor, a novel torsinA-interacting protein implicated in dystonia pathogenesis. J Biol Chem 284:21765–21775.

Glasgow SM, Henke RM, Macdonald RJ, Wright C V, Johnson JE (2005) Ptf1a determines GABAergic over glutamatergic neuronal cell fate in the spinal cord dorsal horn. Development 132:5461–5469 Available at: http://www.ncbi.nlm.nih.gov/pubmed/16291784.

Goodchild RE, Kim CE, Dauer WT (2005) Loss of the dystonia-associated protein torsinA selectively disrupts the neuronal nuclear envelope. Neuron 48:923–932.

Granata A, Koo SJ, Haucke V, Schiavo G, Warner TT (2011) CSN complex controls the stability of selected synaptic proteins via a torsinA-dependent process. EMBO J 30:181–193 Available at: http://dx.doi.org/10.1038/emboj.2010.285.

Granata A, Schiavo G, Warner TT (2009) TorsinA and dystonia: From nuclear envelope to synapse. J Neurochem 109:1596–1609.

Granata A, Watson R, Collinson LM, Schiavo G, Warner TT (2008) The dystonia-associated protein TorsinA modulates synaptic vesicle recycling. J Biol Chem 283:7568–7579.

Gross MK, Dottori M, Goulding M (2002) Lbx1 specifies somatosensory association interneurons in the dorsal spinal cord. Neuron 34:535–549.

Haase G, Dessaud E, Garcès A, De Bovis B, Birling MC, Filippi P, Schmalbruch H, Arber S, DeLapeyrière O (2002) GDNF acts through PEA3 to regulate cell body positioning and muscle innervation of specific motor neuron pools. Neuron 35:893–905.

Hanson MG, Landmesser LT (2003) Characterization of the circuits that generate spontaneous episodes of activity in the early embryonic mouse spinal cord. J Neurosci 23:587–600.

Hantman AW, Jessell TM (2011) Clarke's Column Neurons as the Focus of a Corticospinal Corollary Circuit. Nat Neurosci 13:1233–1239.

Helms AW, Battiste J, Henke RM, Nakada Y, Simplicio N, Guillemot F, Johnson JE (2005) Sequential roles for Mash1 and Ngn2 in the generation of dorsal spinal cord interneurons. Development 132:2709–2719 Available at: http://www.ncbi.nlm.nih.gov/pubmed/15901662.

Helms AW, Johnson JE (2003) Specification of dorsal spinal cord interneurons. Curr Opin Neurobiol 13:42–49.

Hollyday M, Hamburger V (1977) An autoradiographic study of the formation of the lateral motor column in the chick embryo. Brain Res 132:197–208

Available at: http://www.sciencedirect.com/science/article/pii/0006899377904164 [Accessed September 17, 2015].

Hughes DI, Mackie M, Nagy GG, Riddell JS, Maxwell DJ, Szabó G, Erdélyi F, Veress G, Szucs P, Antal M, Todd AJ (2005) P boutons in lamina IX of the rodent spinal cord express high levels of glutamic acid decarboxylase-65 and originate from cells in deep medial dorsal horn. Proc Natl Acad Sci U S A 102:9038–9043 Available at: http://www.ncbi.nlm.nih.gov/pubmed/15947074.

Ilardi JM, Mochida S, Sheng ZH (1999) Snapin: a SNARE-associated protein implicated in synaptic transmission. Nat Neurosci 2:119–124.

Jankowska E (1992) Interneuronal relay in spinal pathways from proprioceptors. Prog Neurobiol 38:335–378 Available at: http://www.sciencedirect.com/science/article/pii/0301008292900249 [Accessed August 21, 2015].

Jankowska E (2001) Spinal interneuronal systems: Identification, multifunctional character and reconfigurations in mammals. J Physiol 533:31–40.

Jankowska E, McCrea D, Rudomín P, Sykova E (1981) Observations on neuronal pathways subserving primary afferent depolarization. J Neurophysiol 46:506–516 Available at: http://www.ncbi.nlm.nih.gov/pubmed/7299431.

Jessell TM (2000) Neuronal specification in the spinal cord: inductive signals and transcriptional codes. Nat Rev Genet 1:20–29.

Jiang S, Seng S, Avraham HK, Fu Y, Avraham S (2007) Process elongation of oligodendrocytes is promoted by the Kelch-related protein MRP2/KLHL1. J Biol Chem 282:12319–12329.

Jiang X, Shen S, Cadwell CR, Berens P, Sinz F, Ecker AS, Patel S, Tolias AS (2015) Principles of connectivity among morphologically defined cell types in adult neocortex. Science (80-) 350:aac9462–aac9462 Available at: http://www.sciencemag.org/cgi/doi/10.1126/science.aac9462.

Jin K, Jiang H, Xiao D, Zou M, Zhu J, Xiang M (2015) Tfap2a and 2b act downstream of Ptf1a to promote amacrine cell differentiation during retinogenesis. Mol Brain 8:28 Available at: http://www.molecularbrain.com/content/8/1/28.

Kawaguchi Y, Cooper B, Gannon M, Ray M, MacDonald RJ, Wright CVE (2002) The role of the transcriptional regulator Ptf1a in converting intestinal to pancreatic progenitors. Nat Genet 32:128–134.

Kepecs A, Fishell G (2014) Interneuron cell types are fit to function. Nature 505:318–326 Available at: http://www.ncbi.nlm.nih.gov/pubmed/24429630.

Kim CE, Perez A, Perkins G, Ellisman MH, Dauer WT (2010) A molecular mechanism underlying the neural-specific defect in torsinA mutant mice. Proc Natl Acad Sci U S A 107:9861–9866.

Knikou M (2008) The H-reflex as a probe: Pathways and pitfalls. J Neurosci Methods 171:1–12.

Konakova M, Pulst SM (2005) Dystonia-associated forms of torsinA are deficient in ATPase activity. J Mol Neurosci 25:105–117.

Kubota Y, Karube F, Nomura M, Kawaguchi Y (2016) The Diversity of Cortical Inhibitory Synapses. Front Neural Circuits 10 Available at: http://www.frontiersin.org/Journal/Abstract.aspx?s=740&name=neural_circuits&ART_DOI=10.3389/fncir.2016.00027.

Ladle DR, Pecho-Vrieseling E, Arber S (2007) Assembly of motor circuits in the spinal cord: driven to function by genetic and experience-dependent mechanisms. Neuron 56:270–283.

Liang CC, Tanabe LM, Jou S, Chi F, Dauer WT (2014) TorsinA hypofunction causes abnormal twisting movements and sensorimotor circuit neurodegeneration. J Clin Invest 124:3080–3092.

Liem KF, Jessell TM, Briscoe J (2000) Regulation of the neural patterning activity of sonic hedgehog by secreted BMP inhibitors expressed by notochord and somites. Development 127:4855–4866.

Lin JH, Saito T, Anderson DJ, Lance-Jones C, Jessell TM, Arber S (1998) Functionally related motor neuron pool and muscle sensory afferent subtypes defined by coordinate ETS gene expression. Cell 95:393–407.

Livet J, Sigrist M, Stroebel S, De Paola V, Price SR, Henderson CE, Jessell TM, Arber S (2002) ETS gene Pea3 controls the central position and terminal arborization of specific motor neuron pools. Neuron 35:877–892.

Lopez-Bendito G, Sturgess K, Erdelyi F, Szabo G, Molnar Z, Paulsen O (2004) Preferential origin and layer destination of GAD65-GFP cortical interneurons. Cereb Cortex 14:1122–1133.

Madisen L, Zwingman TA, Sunkin SM, Oh SW, Zariwala HA, Gu H, Ng LL, Palmiter RD, Hawrylycz MJ, Jones AR, Lein ES, Zeng H (2010) A robust and high-throughput Cre reporting and characterization system for the whole mouse brain. Nat Neurosci 1371:133–140 Available at: http://dx.doi.org/10.1038/nn.2467.

Matise MP, Joyner a L (1997) Expression patterns of developmental control genes in normal and Engrailed-1 mutant mouse spinal cord reveal early diversity in developing interneurons. J Neurosci 17:7805–7816.

McHanwell S, Biscoe TJ (1981) The sizes of motoneurons supplying hindlimb muscles in the mouse. Proc R Soc Lond B Biol Sci 213:201–216.

Mears SC, Frank E (1997) Formation of specific monosynaptic connections between muscle spindle afferents and motoneurons in the mouse. J

Neurosci 17:3128–3135 Available at: http://eutils.ncbi.nlm.nih.gov/entrez/eutils/elink.fcgi?dbfrom=pubmed&id=9096147&retmode=ref&cmd=prlinks\npapers2://publication/uuid/BF819FA0-E38E-4E14-9E43-2181467ACD27.

Mentis GZ, Siembab VC, Zerda R, O'Donovan MJ, Alvarez FJ (2006) Primary afferent synapses on developing and adult Renshaw cells. J Neurosci 26:13297–13310.

Mizuguchi R, Kriks S, Cordes R, Gossler A, Ma Q, Goulding M (2006) Ascl1 and Gsh1/2 control inhibitory and excitatory cell fate in spinal sensory interneurons. Nat Neurosci 9:770–778 Available at: http://www.ncbi.nlm.nih.gov/pubmed/16715081.

Morita H, Crone C, Christenhuis D, Petersen NT, Nielsen JB (2001) Modulation of presynaptic inhibition and disynaptic reciprocal Ia inhibition during voluntary movement in spasticity. Brain:826–837.

Morita H, Shindo M, Ikeda S, Yanagisawa N (2000) Decrease in presynaptic inhibition on heteronymous monosynaptic Ia terminals in patients with Parkinson's disease. Mov Disord 15:830–834.

Müller T, Brohmann H, Pierani A, Heppenstall PA, Lewin GR, Jessell TM, Birchmeier C (2002) The homeodomain factor Lbx1 distinguishes two major programs of neuronal differentiation in the dorsal spinal cord. Neuron 34:551–562.

Nakashima K, Rothwell JC, Day BL, Thompson PD, Shannon K, Marsden CD (1989) Reciprocal inhibition between forearm muscles in patients with writer's cramp and other occupational cramps, symptomatic hemidystonia and hemiparesis due to stroke. Brain 112 (Pt 3:681–697.

Nelson AB, Kreitzer AC (2014) Reassessing models of Basal Ganglia function and dysfunction. Annu Rev Neurosci 37:117–135 Available at: http://www.ncbi.nlm.nih.gov/pubmed/25032493.

Nemes JP, Benzow KA, Moseley ML, Ranum LP, Koob MD (2000) The SCA8 transcript is an antisense RNA to a brain-specific transcript encoding a novel actin-binding protein (KLHL1). Hum Mol Genet 9:1543–1551.

Nguyen MT, Zhu J, Nakamura E, Bao X, Mackem S (2009) Tamoxifen-dependent, inducible Hoxb6CreERT recombinase function in lateral plate and limb mesoderm, CNS isthmic organizer, posterior trunk neural crest, hindgut, and tailbud. Dev Dyn 238:467–474.

Nornes HO, Carry M (1978) Neurogenesis in spinal cord of mouse: an autoradiographic analysis. Brain Res 159:1–16 Available at: http://www.sciencedirect.com/science/article/pii/0006899378901051 [Accessed September 17, 2015].

Ozaki S, Snider WD (1997) Initial trajectories of sensory axons toward laminar targets in the developing mouse spinal cord. J Comp Neurol 380:215–229.

Ozelius LJ, Hewett JW, Page CE, Bressman SB, Kramer PL, Shalish C, de Leon D, Brin MF, Raymond D, Corey DP, Fahn S, Risch NJ, Buckler a J, Gusella JF, Breakefield XO (1997) The early-onset torsion dystonia gene (DYT1) encodes an ATP-binding protein. Nat Genet 17:40–48.

Pan FC, Bankaitis ED, Boyer D, Xu X, Van de Casteele M, Magnuson MA, Heimberg H, Wright CVE (2013) Spatiotemporal patterns of multipotentiality in Ptf1a-expressing cells during pancreas organogenesis and injury-induced facultative restoration. Development 140:751–764 Available at: http://www.ncbi.nlm.nih.gov/pubmed/23325761.

Panizza M, Lelli S, Nilsson J, Hallett M (1990) H-reflex recovery curve and reciprocal inhibition of H-reflex in different kinds of dystonia. Neurology 40:824–828.

Pappas SS, Darr K, Holley SM, Cepeda C, Mabrouk OS, Wong J-MT, LeWitt TM, Paudel R, Houlden H, Kennedy RT, Levine MS, Dauer WT (2015) Forebrain deletion of the dystonia protein torsinA causes dystonic-like movements and loss of striatal cholinergic neurons. Elife 4 Available at: http://www.pubmedcentral.nih.gov/articlerender.fcgi?artid=4473728&tool=pmcentrez&rendertype=abstract.

Pecho-Vrieseling E, Sigrist M, Yoshida Y, Jessell TM, Arber S (2009) Specificity of sensory-motor connections encoded by Sema3e-Plxnd1 recognition. Nature 459:842–846 Available at: http://pubs.acs.org/doi/abs/10.1021/ac901991x.

Perissinotti PP, Ethington EA, Almazan E, Martinez-Hernandez E, Kalil J, Koob MD, Piedras-Renteria ES (2015) Calcium current homeostasis and synaptic deficits in hippocampal neurons from Kelch-like 1 knockout mice. Front Cell Neurosci 8:1–12 Available at: http://journal.frontiersin.org/article/10.3389/fncel.2014.00444/abstract.

Pham P, Frei KP, Woo W, Truong DD (2006) Molecular defects of the dystonia-causing torsinA mutation. Neuroreport 17:1725–1728 Available at: http://www.ncbi.nlm.nih.gov/pubmed/17047461.

Polgar E, Durrieux C, Hughes DI, Todd AJ (2013) A quantitative study of inhibitory interneurons in laminae I-III of the mouse spinal dorsal horn. PLoS One 8:e78309 Available at: http://www.ncbi.nlm.nih.gov/pubmed/24205193.

Priori A, Berardelli A, Mercuri B, Manfredi M (1995) Changes in reciprocal inhibition between forearm muscles. Brain:801–807.

Priori A, Polidori L, Rona S, Manfredi M, Berardelli A (2000) Spinal and cortical inhibition in Huntington's chorea. Mov Disord 15:938–946.

Puglisi F, Vanni V, Ponterio G, Tassone A, Sciamanna G, Bonsi P, Pisani A, Mandolesi G (2013) Torsin A Localization in the Mouse Cerebellar Synaptic Circuitry. PLoS One 8:1–16.

Réthelyi M, Light AR, Perl ER (1982) Synaptic complexes formed by

functionally defined primary afferent units with fine myelinated fibers. J Comp Neurol 207:381–393.

Roberts RC, Part NJ, Farquhar R, Butchart P (1994) Presynaptic inhibition of soleus Ia afferent terminals in Parkinson's disease. J Neurol Neurosurg Psychiatry 57:1488–1491 Available at: http://jnnp.bmj.com/cgi/content/abstract/jnnp\n57/12/1488.

Roelink H, Porter J a, Chiang C, Tanabe Y, Chang DT, Beachy P a, Jessell TM (1995) Floor plate and motor neuron induction by different concentrations of the amino-terminal cleavage product of sonic hedgehog autoproteolysis. Cell 81:445–455.

Romanes GJ (1951) The motor cell columns of the lumbo-sacral spinal cord of the cat. J Comp Neurol 94:313–363 Available at: http://dx.doi.org/10.1002/cne.900940209.

Rudomin, P. & Schmidt RF (1999) Presynaptic inhibition in the verbetrate spinal cord revisited. Exp Brain Res:1–37.

Rudomin P (2009) In search of lost presynaptic inhibition. Exp Brain Res 196:139–151.

Russ JB, Borromeo MD, Kollipara RK, Bommareddy PK, Johnson JE, Kaltschmidt JA (2015) Misexpression of Ptf1a in Cortical Pyramidal Cells In Vivo Promotes an Inhibitory Peptidergic Identity. J Neurosci 35:6028–6037.

Russ JB, Verina T, Comer JD, Comi AM, Kaltschmidt JA (2013) Corticospinal tract insult alters GABAergic circuitry in the mammalian spinal cord. Front Neural Circuits 7:150 Available at: http://www.pubmedcentral.nih.gov/articlerender.fcgi?artid=3782692&tool=pmcentrez&rendertype=abstract.

Sciamanna G, Tassone a., Mandolesi G, Puglisi F, Ponterio G, Martella G, Madeo G, Bernardi G, Standaert DG, Bonsi P, Pisani a. (2012) Cholinergic Dysfunction Alters Synaptic Integration between Thalamostriatal and Corticostriatal Inputs in DYT1 Dystonia. J Neurosci 32:11991–12004.

Seng S, Avraham HK, Jiang S, Venkatesh S, Avraham S (2006) KLHL1/MRP2 mediates neurite outgrowth in a glycogen synthase kinase 3beta-dependent manner. Mol Cell Biol 26:8371–8384 Available at: http://www.pubmedcentral.nih.gov/articlerender.fcgi?artid=1636797&tool=pmcentrez&rendertype=abstract.

Sharma N (2005) Impaired Motor Learning in Mice Expressing TorsinA with the DYT1 Dystonia Mutation. J Neurosci 25:5351–5355 Available at: http://www.jneurosci.org/cgi/doi/10.1523/JNEUROSCI.0855-05.2005.

Shashidharan P, Kramer BC, Walker RH, Olanow CW, Brin MF (2000) Immunohistochemical localization and distribution of torsinA in normal human and rat brain. Brain Res 853:197–206.

Stam FJ, Hendricks TJ, Zhang J, Geiman EJ, Francius C, Labosky P a., Clotman F, Goulding M (2012) Renshaw cell interneuron specialization is controlled by a temporally restricted transcription factor program. Development 139:179–190.

Stifani N (2014) Motor neurons and the generation of spinal motor neuron diversity. Front Cell Neurosci 8:293 Available at: http://journal.frontiersin.org/article/10.3389/fncel.2014.00293/abstract.

Sürmeli G, Akay T, Ippolito GC, Tucker PW, Jessell TM (2011) Patterns of spinal sensory-motor connectivity prescribed by a dorsoventral positional template. Cell 147:653–665.

Tillakaratne NJ, Mouria M, Ziv NB, Roy RR, Edgerton VR, Tobin a J (2000) Increased expression of glutamate decarboxylase (GAD(67)) in feline lumbar spinal cord after complete thoracic spinal cord transection. J Neurosci Res 60:219–230 Available at: http://www.ncbi.nlm.nih.gov/pubmed/10740227.

Todd AJ (1996) GABA and glycine in synaptic glomeruli of the rat spinal dorsal horn. Eur J Neurosci 8:2492–2498 Available at: http://www.ncbi.nlm.nih.gov/pubmed/8996798.

Todd AJ (2010) Neuronal circuitry for pain processing in the dorsal horn. Nat Rev Neurosci 11:823–836.

Tripodi M, Stepien AE, Arber S (2011) Motor antagonism exposed by spatial segregation and timing of neurogenesis. Nature 479:61–66 Available at: http://www.ncbi.nlm.nih.gov/pubmed/22012263.

Vanni V, Puglisi F, Bonsi P, Ponterio G, Maltese M, Pisani A, Mandolesi G (2015) Cerebellar synaptogenesis is compromised in mouse models of DYT1 dystonia. Exp Neurol 271:457–467 Available at: http://dx.doi.org/10.1016/j.expneurol.2015.07.005.

Vrieseling E, Arber S (2006) Target-Induced Transcriptional Control of Dendritic Patterning and Connectivity in Motor Neurons by the ETS Gene Pea3. Cell 127:1439–1452.

Watson a. HD (2003) GABA- and glycine-like immunoreactivity in axons and dendrites contacting the central terminals of rapidly adapting glabrous skin afferents in rat spinal cord. J Comp Neurol 464:497–510.

Watson AH, Hughes DI, Bazzaz AA (2002) Synaptic relationships between hair follicle afferents and neurones expressing GABA and glycine-like immunoreactivity in the spinal cord of the rat. J Comp Neurol 452:367–380 Available at: http://www.ncbi.nlm.nih.gov/pubmed/12355419.

Welniarz Q, Dusart I, Gallea C, Roze E (2015) One hand clapping: lateralization of motor control. Front Neuroanat 9:75 Available at: http://www.pubmedcentral.nih.gov/articlerender.fcgi?artid=4451425&tool=pmcentrez&rendertype=abstract.

Wildner H, Das Gupta R, Bröhl D, Heppenstall PA, Zeilhofer HU, Birchmeier C (2013) Genome-wide expression analysis of Ptf1a- and Ascl1-deficient mice reveals new markers for distinct dorsal horn interneuron populations contributing to nociceptive reflex plasticity. J Neurosci 33:7299–7307 Available at: http://www.ncbi.nlm.nih.gov/pubmed/23616538.

Wildner H, Müller T, Cho S-H, Bröhl D, Cepko CL, Guillemot F, Birchmeier C (2006) dILA neurons in the dorsal spinal cord are the product of terminal and non-terminal asymmetric progenitor cell divisions, and require Mash1 for their development. Development 133:2105–2113.

Windhorst U (1996) On the role of recurrent inhibitory feedback in motor control. Prog Neurobiol 49:517–587.

Wistow G, Kim H (1991) Lens protein expression in mammals: Taxon-specificity and the recruitment of crystallins. J Mol Evol 32:262–269.

Yokoi F, Cheetham CC, Campbell SL, Sweatt JD, Li Y (2013) Pre-Synaptic Release Deficits in a DYT1 Dystonia Mouse Model. PLoS One 8:e72491 Available at: http://dx.plos.org/10.1371/journal.pone.0072491.

Yokoi F, Chen H-X, Dang MT, Cheetham CC, Campbell SL, Roper SN, Sweatt JD, Li Y (2015) Behavioral and Electrophysiological Characterization of Dyt1 Heterozygous Knockout Mice. PLoS One 10:e0120916 Available at: http://dx.plos.org/10.1371/journal.pone.0120916.

Zeilhofer HU, Wildner H, Yevenes GE (2012) Fast Synaptic Inhibition in Spinal Sensory Processing and Pain Control. Physiol Rev 92:193–235.